

A peer-reviewed version of this preprint was published in PeerJ on 29 August 2018.

[View the peer-reviewed version](https://doi.org/10.7717/peerj.5518) (peerj.com/articles/5518), which is the preferred citable publication unless you specifically need to cite this preprint.

Hengl T, Nussbaum M, Wright MN, Heuvelink GBM, Gräler B. 2018. Random forest as a generic framework for predictive modeling of spatial and spatio-temporal variables. PeerJ 6:e5518
<https://doi.org/10.7717/peerj.5518>

1 Random Forest as a Generic Framework for 2 Predictive Modeling of Spatial and 3 Spatio-temporal Variables

4 Tomislav Hengl¹, Madlene Nussbaum², Marvin N. Wright³, and Gerard
5 B.M. Heuvelink⁴

6 ¹Envirometrix Ltd., Wageningen, the Netherlands

7 ²Bern University of Applied Sciences BFH, School of Agricultural, Forest and Food
8 Sciences HAFL, Zollikofen, Bern, Switzerland

9 ³Leibniz Institute for Prevention Research and Epidemiology — BIPS, Bremen, Germany

10 ⁴ISRIC – World Soil Information and Soil Geography and Landscape group,
11 Wageningen University, Wageningen, the Netherlands

12 Corresponding author:

13 Tomislav Hengl¹

14 Email address: tom.hengl@gmail.com

15 ABSTRACT

16 Random forest and similar Machine Learning techniques are already used to generate spatial predictions,
17 but spatial location of points (geography) is often ignored in the modeling process. Spatial auto-correlation,
18 especially if still existent in the cross-validation residuals, indicates that the predictions are maybe biased, and
19 this is suboptimal. This paper presents a random forest for spatial predictions framework ("RFsp") where
20 buffer distances from observation points are used as explanatory variables, thus incorporating geographical
21 proximity effects into the prediction process. The "RFsp" framework is illustrated with examples that
22 use textbook datasets and apply spatial and spatio-temporal prediction to numeric, binary, categorical,
23 multivariate and spatiotemporal variables. Performance of the RFsp framework is compared with the
24 state-of-the-art kriging techniques using 5-fold cross-validation with refitting. The results show that RFsp
25 can obtain equally accurate and unbiased predictions as different versions of kriging. Advantages of using
26 RFsp over kriging are that it needs no rigid statistical assumptions about the distribution and stationarity
27 of the target variable, it is more flexible towards incorporating, combining and extending covariates of
28 different types, and it possibly yields more informative maps characterizing the prediction error. RFsp
29 appears to be especially attractive for building multivariate spatial prediction models that can be used as
30 'knowledge engines' in various geoscience fields. Some disadvantages of RFsp are the exponentially growing
31 computational intensity with increase of calibration data and covariates and the high sensitivity of predictions
32 to input data quality. For many data sets, especially those with lower number of points and covariates and
33 close-to-linear relationships, model-based geostatistics can still lead to more accurate predictions than RFsp.

Submitted to PeerJ on 27th of February 2018

INTRODUCTION

Kriging and its many variants have been used for spatial interpolation since the 1960's (Isaaks and Srivastava, 1989; Cressie, 1990; Goovaerts, 1997) and have proven on numerous occasions to be superior to more simplistic deterministic interpolation techniques. The number of published applications on kriging has steadily increased since 1980 and the technique is now used in a variety of fields, ranging from physical geography (Oliver and Webster, 1990), geology and soil science (Goovaerts, 1999; Minasny and McBratney, 2007), hydrology (Skøien et al., 2005), epidemiology (Moore and Carpenter, 1999; Graham et al., 2004), natural hazard monitoring (Dubois, 2005) and climatology (Hudson and Wackernagel, 1994; Hartkamp et al., 1999). One of the reasons why kriging has been used so widely is its accessibility to researchers, especially thanks to the makers of gslib (Deutsch and Journel, 1998), ESRI's Geostatistical Analyst (www.esri.com), ISATIS (www.geovariances.com) and developers of the gstat (Pebesma, 2004; Bivand et al., 2008), geoR (Diggle and Ribeiro Jr, 2007) and geostatsp (Brown, 2015) packages for R.

Since the start of the 21st century, however, there has been an increasing interest in using more computationally intensive and primarily data-driven algorithms. These techniques are also known under the name "*machine learning*", and are applicable for various data mining, pattern recognition, regression and classification problems. One of the machine learning algorithms (MLA) that has recently proven to be efficient for producing spatial predictions is the random forest algorithm, first described in Breiman (2001), and now available also in a fast scalable implementation through the ranger package for R (Wright and Ziegler, 2017). Several studies (Prasad et al., 2006; Hengl et al., 2015; Vaysse and Lagacherie, 2015; Nussbaum et al., 2017a) have already shown that random forest is a promising technique for spatial prediction. Random forest, however, ignores the spatial locations of the observations and hence any spatial autocorrelation in the data not accounted for by the covariates. Modeling the relationship with covariates and spatial autocorrelation jointly using machine learning techniques is relatively novel and not entirely worked out. Using northing and easting as covariates in a random forest model may not help the prediction process as it leads to linear features and discrete boundaries (obvious artifacts) which are directly related to the configuration of the sampling plan. A more sensible and worked-out use of geographical space is needed.

In this paper we describe a generic framework for spatial and spatiotemporal prediction that is based on random forest and which we refer to as "*RFsp*". With this framework we aim at including information derived from the observation locations and their spatial distribution into predictive modeling. We test whether RFsp, and potentially other tree-based machine learning algorithms, can be used as a replacement for geostatistical interpolation techniques such as ordinary and regression-kriging, i.e., kriging with external drift. We explain in detail (using standard data sets) how to extend machine learning to general spatial prediction, and compare the prediction efficiency of random forest with that of state-of-the-art kriging methods using 5-fold cross-validation with refitting the model in each subset.

A complete benchmarking of the prediction efficiency is documented in R code and can be obtained via the GitHub repository at <https://github.com/thengl/GeoMLA>. All datasets used in this paper

are either part of an existing R package or can be obtained from the GitHub repository.

METHODS AND MATERIALS

Spatial Prediction

Spatial prediction is concerned with the prediction of the occurrence, quantity and/or state of geographical phenomena, usually based on training data, e.g., ground measurements or samples $y(\mathbf{s}_i), i = 1 \dots n$, where $\mathbf{s}_i \in \mathbf{D}$ is a spatial coordinate (i.e., easting and northing), n is the number of observed locations and \mathbf{D} is the geographical domain. Spatial prediction typically results in gridded maps or, in case of space-time prediction, animated visualizations of spatiotemporal phenomena.

Model-based spatial prediction algorithms commonly aim to minimize the prediction error variance $\sigma^2(\mathbf{s}_0)$ at a prediction location \mathbf{s}_0 under the constraint of unbiasedness (Christensen, 2001). Unbiasedness and prediction error variance are defined in terms of a statistical model $Y = \{Y(\mathbf{s}), \mathbf{s} \in \mathbf{D}\}$ of y . In mathematical terms, the prediction error variance:

$$\sigma^2(\mathbf{s}_0) = E \left\{ \left(\hat{Y}(\mathbf{s}_0) - Y(\mathbf{s}_0) \right)^2 \right\} \quad (1)$$

is to be minimized while satisfying the (unbiasedness) constraint:

$$E \left\{ \hat{Y}(\mathbf{s}_0) - Y(\mathbf{s}_0) \right\} = 0 \quad (2)$$

The predictor $\hat{Y}(\mathbf{s}_0)$ of $Y(\mathbf{s}_0)$ is typically taken as a function of covariates and the $Y(\mathbf{s}_i)$ which, upon substitution of the observations $y(\mathbf{s}_i)$, yields a (deterministic) prediction $\hat{y}(\mathbf{s}_0)$.

The spatial prediction process is repeated at all nodes of a grid covering \mathbf{D} (or a space-time domain in case of spatio-temporal prediction) and produces three main outputs:

1. Estimates of the model parameters (e.g., regression coefficients and variogram parameters), i.e., the **model**;
2. Predictions at new locations, i.e., a **prediction map**;
3. Estimate of uncertainty associated with the predictions, i.e., a **prediction error variance map**.

In the case of multiple linear regression (MLR), model assumptions state that at any location in \mathbf{D} the dependent variable is the sum of a linear combination of the covariates at that location and a zero-mean normally distributed residual. Thus, at the n observation locations we have:

$$\mathbf{Y} = \mathbf{X}^T \cdot \boldsymbol{\beta} + \boldsymbol{\varepsilon}, \quad (3)$$

where \mathbf{Y} is a vector of the target variable at the n observation locations, \mathbf{X} is an $n \times p$ matrix of covariates at the same locations and $\boldsymbol{\beta}$ is a vector of p regression coefficients. The stochastic residual $\boldsymbol{\varepsilon}$ is assumed to

be independently and identically distributed. The paired observations of the target variable and covariates (\mathbf{y} and \mathbf{X}) are used to estimate the regression coefficients using, e.g., Ordinary Least Squares (Kutner et al., 2004):

$$\hat{\beta} = (\mathbf{X}^T \cdot \mathbf{X})^{-1} \cdot \mathbf{X}^T \cdot \mathbf{y} \quad (4)$$

once the coefficients are estimated these can be used to generate a prediction at \mathbf{s}_0 :

$$\hat{y}(\mathbf{s}_0) = \mathbf{x}_0^T \cdot \hat{\beta} \quad (5)$$

with associated prediction error variance:

$$\sigma^2(\mathbf{s}_0) = \text{var}(\varepsilon(\mathbf{s}_0)) \cdot \left[1 + \mathbf{x}_0^T \cdot (\mathbf{X}^T \cdot \mathbf{X})^{-1} \cdot \mathbf{x}_0 \right] \quad (6)$$

here, \mathbf{x}_0 is a vector with covariates at the prediction location and $\text{var}(\varepsilon(\mathbf{s}_0))$ is the variance of the stochastic residual. The latter is usually estimated by the mean squared error (MSE):

$$\text{MSE} = \frac{\sum_{i=1}^n (y_i - \hat{y}_i)^2}{n - p} \quad (7)$$

The prediction error variance given by Eq. (6) is smallest at prediction points where the covariate values are in the center of the covariate ('feature') space and increases as predictions are made further away from the center. They are particularly large in case of extrapolation in feature space (Kutner et al., 2004). Note that the model defined in Eq. (3) is basically a non-spatial model because the observation locations and spatial-autocorrelation of the dependent variable are not taken into account.

Kriging

Kriging is a technique developed specifically to employ knowledge about spatial autocorrelation in modeling and prediction (Matheron, 1969; Christensen, 2001; Oliver and Webster, 2014). Most geostatistical models assume that the target variable Y at some geographic location \mathbf{s} can be modeled as the sum of a deterministic mean (μ) and a stochastic residual (ε) (Goovaerts, 1997; Cressie, 2015):

$$Y(\mathbf{s}) = \mu(\mathbf{s}) + \varepsilon(\mathbf{s}) \quad (8)$$

Assuming a constant trend ($\mu(\mathbf{s}) = \mu$ for all $\mathbf{s} \in \mathbf{D}$), the best linear unbiased prediction (BLUP) of

$y(\mathbf{s}_0)$ is given by the ordinary kriging (OK) prediction (Goovaerts, 1997):

$$\hat{y}_{OK}(\mathbf{s}_0) = \mathbf{w}(\mathbf{s}_0)^T \cdot \mathbf{y} \quad \text{with} \quad \mathbf{w}(\mathbf{s}_0)^T \cdot \mathbf{1} = \sum_{i=1}^n w_i(\mathbf{s}_0) = 1, \quad (9)$$

where $\mathbf{w}(\mathbf{s}_0)^T$ is a vector of kriging weights $w_i(\mathbf{s}_0)$. These are obtained by solving a linear set of equations (Goovaerts, 1997; Cressie, 2015):

$$\begin{bmatrix} C(\mathbf{s}_1, \mathbf{s}_1) & \cdots & C(\mathbf{s}_1, \mathbf{s}_n) & 1 \\ \vdots & & \vdots & \vdots \\ C(\mathbf{s}_n, \mathbf{s}_1) & \cdots & C(\mathbf{s}_n, \mathbf{s}_n) & 1 \\ 1 & \cdots & 1 & 0 \end{bmatrix} \cdot \begin{bmatrix} w_1(\mathbf{s}_0) \\ \vdots \\ w_n(\mathbf{s}_0) \\ \varphi \end{bmatrix} = \begin{bmatrix} C(\mathbf{s}_0, \mathbf{s}_1) \\ \vdots \\ C(\mathbf{s}_0, \mathbf{s}_n) \\ 1 \end{bmatrix} \quad (10)$$

where $C(\mathbf{s}_i, \mathbf{s}_j) = \text{cov}(Y(\mathbf{s}_i), Y(\mathbf{s}_j))$ and φ is a Lagrange multiplier.

The associated prediction error variance, i.e., the OK variance, is given by (Webster and Oliver, 2001, p.183):

$$\sigma_{OK}^2(\mathbf{s}_0) = \text{var}(Y(\mathbf{s}_0) - \hat{Y}(\mathbf{s}_0)) = C(\mathbf{s}_0, \mathbf{s}_0) - \mathbf{w}(\mathbf{s}_0)^T \cdot \mathbf{C}_0 - \varphi, \quad (11)$$

where \mathbf{C}_0 is an n -vector of covariances between $Y(\mathbf{s}_0)$ and the $Y(\mathbf{s}_i)$.

If the distribution of the target variable is not Gaussian, a transformed Gaussian approach (Diggle and Ribeiro Jr, 2007, §3.8) and/or generalized linear geostatistical model approach (Brown, 2015) is required. For example, the Box-Cox family of transformations is often recommended for skewed data (Diggle and Ribeiro Jr, 2007):

$$Y_T = \begin{cases} (Y^\eta - 1)/\eta & \text{if } \eta \neq 0 \\ \log(Y) & \text{if } \eta = 0, \end{cases} \quad (12)$$

where η is the Box-Cox transformation parameter and Y_T is the transformed target variable. The prediction and prediction error variance for log-normal OK ($\eta = 0$) are back-transformed using (Diggle and Ribeiro Jr, 2007, p.61):

$$\hat{y}(\mathbf{s}_0) = \exp[\hat{y}_T(\mathbf{s}_0) + 0.5 \cdot \sigma_T^2(\mathbf{s}_0)] \quad (13)$$

$$\sigma^2(\mathbf{s}_0) = \exp[2 \cdot \hat{y}_T(\mathbf{s}_0) + \sigma_T^2(\mathbf{s}_0)] \cdot (\exp[\sigma_T^2(\mathbf{s}_0)] - 1) \quad (14)$$

where $\sigma_T^2(\mathbf{s}_0)$ is the kriging variance on the transformed scale.

The advantages of kriging are (Webster and Oliver, 2001; Christensen, 2001; Oliver and Webster,

133 2014):

- 134 • it takes a comprehensive statistical model as a starting point and derives the optimal prediction for
- 135 this assumed model in a theoretically sound way;
- 136 • it exploits spatial autocorrelation in the variable of interest;
- 137 • it provides a spatially explicit measure of prediction uncertainty.

138 A natural extension of MLR and OK is to combine the two approaches and allow that the MLR
 139 residual of Eq. (3) is spatially correlated. This boils down to “Regression-Kriging” (RK) also known
 140 under names “Universal Kriging” (UK) and/or “Kriging with External Drift” (KED) (Goldberger, 1962;
 141 Goovaerts, 1997; Christensen, 2001; Hengl et al., 2007a). UK/KED implementations are available in most
 142 geostatistical software packages (e.g., geoR and gstat), while the RK approach implies that regression
 143 and kriging are done separately. Both paths are mathematically equivalent i.e. they lead to the same
 144 predictions assuming the same settings are used. The main steps of RK are:

- 145 1. Select and prepare candidate covariates, i.e., maps of environmental and other variables that are
- 146 expected to be correlated with the target variable.
- 147 2. Fit a multiple linear regression model using common procedures, while avoiding collinearity and
- 148 ensuring that the MLR residuals are sufficiently normal. If required use different type of GLM
- 149 (Generalized Linear Model) to account for distribution of the target variable. If covariates are
- 150 strongly correlated it may be advisable to convert these first to principal components.
- 151 3. Derive regression residuals at observation locations and fit a (residual) variogram.
- 152 4. Apply the MLR model at all prediction locations.
- 153 5. Krige the MLR residuals to all prediction locations.
- 154 6. Add up the results of steps 4 and 5.
- 155 7. Apply a back-transformation if needed.

156 The RK algorithm has been very successful over the past decades and is still the mainstream geostatis-
 157 tical technique for generating spatial predictions (Li and Heap, 2011). However, there are five serious
 158 limitations of ordinary and/or regression-kriging:

- 159 1. Kriging assumes that the residuals are normally distributed. This can often be resolved with a
- 160 transformation and back-transformation, but not always. Model-based geostatistics has, at the
- 161 moment, only limited solutions for zero-inflated, Poisson, binomial and other distributions that
- 162 cannot easily be transformed to normality.
- 163 2. Kriging assumes that the residuals are stationary, meaning that these must have a constant mean
- 164 (i.e. zero), constant variance and spatial autocorrelation that only depends on distance.

- 165 3. Kriging also assumes that the variogram is known without error, i.e. it ignores variogram estimation
166 errors (Christensen, 2001, p.286–287). This can be avoided by taking a Bayesian geostatistical
167 approach, but this complicates the analysis considerably (Diggle and Ribeiro Jr, 2007).
- 168 4. Most versions of kriging assume that the relation between dependent and covariates is linear,
169 although some flexibility is offered by including transformed covariates.
- 170 5. In case of numerous possibly correlated covariates, it is very tedious to find a plausible trend
171 model (see, e.g. Nussbaum et al. (2017b)). Interactions among covariates are often difficult to
172 accommodate, and usually lead to an explosion of the number of model parameters.
- 173 6. Kriging can, in the end, be computationally demanding, especially if the number of observations
174 and/or the number of prediction locations is large.

175 Random forest

176 Random forest (RF) (Breiman, 2001; Prasad et al., 2006; Biau and Scornet, 2016) is an extension of
177 bagged trees. It has been primarily used for classification problems and several benchmarking studies
178 have proven that it is one of the best machine learning techniques currently available (Cutler et al., 2007;
179 Boulesteix et al., 2012; Olson et al., 2017).

180 In essence, RF is a data-driven statistical method. The mathematical formulation of the method is
181 rather simple and instead of putting emphasis on formulating a statistical model (Fig. 1), emphasis is
182 put on iteratively training the algorithm, using techniques such as bagging, until a “strong learner” is
183 produced.

184 Predictions in RF are generated as an ensemble estimate from a number of decision trees based on
185 bootstrap samples (bagging). The final predictions are the average of predictions of individual trees
186 (Breiman, 2001; Prasad et al., 2006; Biau and Scornet, 2016):

$$\hat{\theta}^B(x) = \frac{1}{B} \cdot \sum_{b=1}^B t_b^*(x), \quad (15)$$

187 where b is the individual bootstrap sample, B is the total number of trees, and t_b^* is the individual learner,
188 i.e., the individual decision tree:

$$t_b^*(x) = t(x; z_{b1}^*, \dots, z_{bK}^*), \quad (16)$$

189 where z_{bk}^* ($k = 1 \dots K$) is the k -th training sample with pairs of values for the target variable (y) and
190 covariates (x): $z_{bi}^* = (x_k, y_k)$.

191 RF, as implemented in the ranger package, has several parameters that can be fine-tuned. The most
192 important parameters are (Probst and Boulesteix, 2017):

- 193 • mtry — number of variables to possibly split at in each node.

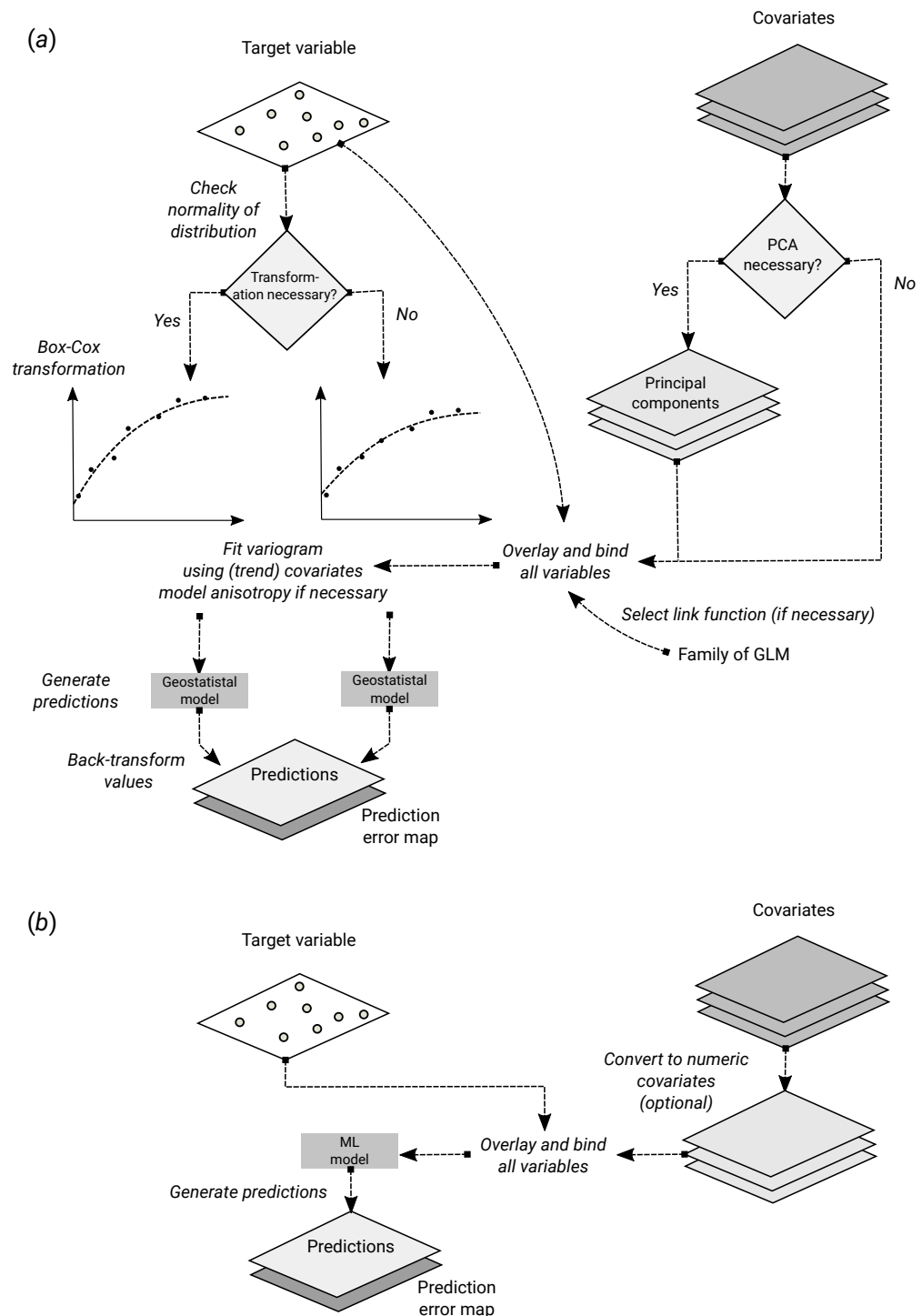


Figure 1. Schematic difference between (a) Kriging with External Drift as implemented in the geor package, and (b) random forest for spatial prediction. Being a mainly data-driven algorithm, random forest requires only limited input from the user, while model-based geostatistics requires variogram modeling, anisotropy modeling, possibly transformation of the target variable and covariates and choice of a link function.

- 194 • `min.node.size` — minimal terminal node size.
- 195 • `sample.fraction` — fraction of observations to sample in each tree.
- 196 • `num.trees` — number of trees.

197 The number of trees in RF does not really need to be fine-tuned, it is recommended to set it to a
198 computationally feasible large number (Lopes, 2015; Probst and Boulesteix, 2017).

199 **Uncertainty of predictions in random forest**

200 The uncertainty of the predictions of random forest for regression-type problems can be estimated using
201 several approaches:

- 202 • The Jackknife-after-Bootstrap method (see e.g. Wager et al. (2014)).
- 203 • The U-statistics approach of Mentch and Hooker (2016).
- 204 • The Monte Carlo simulations (both target variable and covariates) approach of Coulston et al.
205 (2016).
- 206 • The Quantile Regression Forests (QRF) method (Meinshausen, 2006).

207 The approaches by Wager et al. (2014) and Mentch and Hooker (2016) estimate standard errors of the
208 expected values of predictions, used to construct confidence intervals, while the approaches of Coulston
209 et al. (2016) and Meinshausen (2006) estimate prediction intervals. Our primary interest in this article is
210 in the uncertainty of single predictions, and thus we focus on the approach of Meinshausen (2006).

211 The Quantile Regression Forests (QRF) algorithm estimates the quantiles of the distribution of the
212 target variable at prediction points. Thus, the 0.025 and 0.975 quantile may be used to derive the lower
213 and upper limits of a symmetric 95 % prediction interval. It does so by first deriving the random forest
214 prediction algorithm in the usual way. While this is done with decision trees, as explained above, it
215 ultimately boils down to a weighed linear combination of the observations:

$$\hat{y}(\mathbf{s}_0) = \sum_{i=1}^n \alpha_i(\mathbf{s}_0) \cdot y(\mathbf{s}_i) \quad (17)$$

216 in QRF, this equation is used to estimate the cumulative distribution $F_{\mathbf{s}_0}$ of $Y(\mathbf{s}_0)$, conditional to the
217 covariates, simply by replacing the observations $y(\mathbf{s}_i)$ by an indicator transform:

$$\hat{F}_{\mathbf{s}_0}(t) = \sum_{i=1}^n \alpha_i(\mathbf{s}_0) \cdot 1_{y(\mathbf{s}_i) \leq t} \quad (18)$$

218 where $1_{y(\mathbf{s}_i) \leq t}$ is the indicator function (i.e., it is 1 if the condition is true and 0 otherwise). Any quantile q
219 of the distribution can then be derived by iterating towards the threshold t for which $\hat{F}_{\mathbf{s}_0}(t) = q$. Since the
220 entire conditional distribution can be derived in this way, it is also easy to compute the prediction error
221 variance. For details of the algorithm, and a proof of the consistency, see Meinshausen (2006).

Note that in RF and QRF the prediction and associated prediction interval are derived purely using feature space and bootstrap samples. Geographical space is not included in the model as in ordinary and regression-kriging.

Random forest for spatial data (RFsp)

RF is in essence a non-spatial approach to spatial prediction in a sense that sampling locations and general sampling pattern are ignored during the estimation of MLA model parameters. This can potentially lead to sub-optimal predictions and possibly systematic over- or underprediction, especially where the spatial autocorrelation in the target variable is high and where point patterns show clear sampling bias. To overcome this problem we propose the following generic “*RFsp*” system:

$$Y(s) = f(\mathbf{X}_G, \mathbf{X}_R, \mathbf{X}_P) \quad (19)$$

where \mathbf{X}_G are covariates accounting for geographical proximity and spatial relations between observations (to mimic spatial correlation used in kriging), \mathbf{X}_R are surface reflectance covariates, i.e., usually spectral bands of remote sensing images, and \mathbf{X}_P are process-based covariates. For example, the Landsat infrared band is a surface reflectance covariate, while the topographic wetness index and soil weathering index are process-based covariates. Assuming that the RFsp is fitted only using the \mathbf{X}_G , the predictions will likely look similar to OK. If all covariates are used (Eq.19), RFsp will likely produce similar results as regression-kriging.

Geographical covariates

One of the key principles of geography is that “*everything is related to everything else, but near things are more related than distant things*” (Miller, 2004). This principle forms the basis of geostatistics, which converts this rule into a mathematical model, i.e., through spatial autocorrelation functions or variograms. The key to making RF applicable to spatial statistics problems hence lies also in preparing geographical measures of proximity and connectivity between observations, so that spatial autocorrelation is accounted for. There are multiple options for quantifying proximity and geographical connection (Fig. 2):

1. Geographical coordinates s_1 and s_2 , i.e., easting and northing.
2. Euclidean distances to reference points in the study area. For example, distance to the center and edges of the study area, etc.
3. Euclidean distances to sampling locations, i.e., distances from observation locations. Here one buffer distance map can be generated per observation point or group of points. These are also distance measures used in geostatistics.
4. Visibility distances or indices: for each sampling point one can derive the visibility distance and or index (0–100 %) given a Digital Elevation Model (DEM) of the study area. In a highly dissected terrain, points that fall in steep valleys will thus not be visible from all other locations. Visibility distances can be derived using, e.g., SAGA GIS via the Visibility module (Conrad et al., 2015).

255 5. Downslope distances, i.e., distances within a watershed: for each sampling point one can derive
256 upslope/downslope distances to the ridges and hydrological network. This requires, on top of using
257 a Digital Elevation Model, a hydrological analysis of the terrain.

258 6. Resistance distances or weighted buffer distances, i.e., distances of the cumulative effort.

259 The package `gdistance`, for example, provides a framework to derive complex distances based on terrain
260 complexity (van Etten, 2017). Here additional input to compute complex distances are the Digital
261 Elevation Model (DEM) and DEM-derivatives, such as slope (Fig. 2).

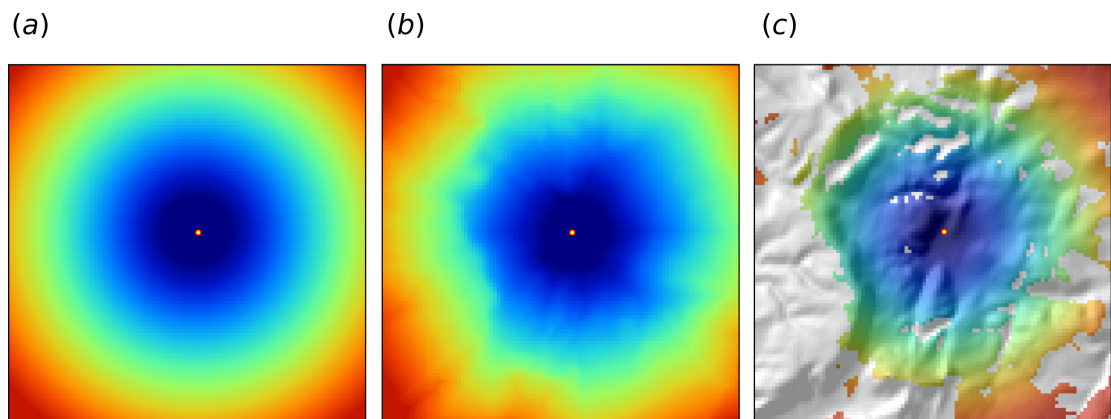


Figure 2. Examples of distance maps based on different derivation algorithms: (a) simple Euclidean distances, (b) complex speed-based distances based on the `gdistance` package and Digital Elevation Model (DEM) (van Etten, 2017), and (c) visibility distance based on the DEM derived in SAGA GIS (Conrad et al., 2015).

262 In this paper we only use geographical coordinates and buffer distances to all sampling points to
263 improve RFsp predictions, but the code we provide could be easily adopted to include other families of
264 geographical covariates, although this would further increase the computational complexity.

265 Model performance criteria

266 When comparing performance of RFsp vs. OK and RK, we use the following performance criteria (Fig. 3):

- 267 1. Average RMSE based on cross-validation (CV) and model R-square — this quantifies the average
268 accuracy of predictions i.e. amount of variation explained.
- 269 2. Average ME based on CV — this quantifies average bias in predictions.
- 270 3. Spatial autocorrelation in CV residuals, i.e., the ratio between nugget and sill variance in the
271 residuals — this quantifies local spatial bias in predictions.
- 272 4. Standard deviation of z -scores — this quantifies the reliability of estimated prediction error vari-
273 ances.

274 The RMSE and ME are derived as:

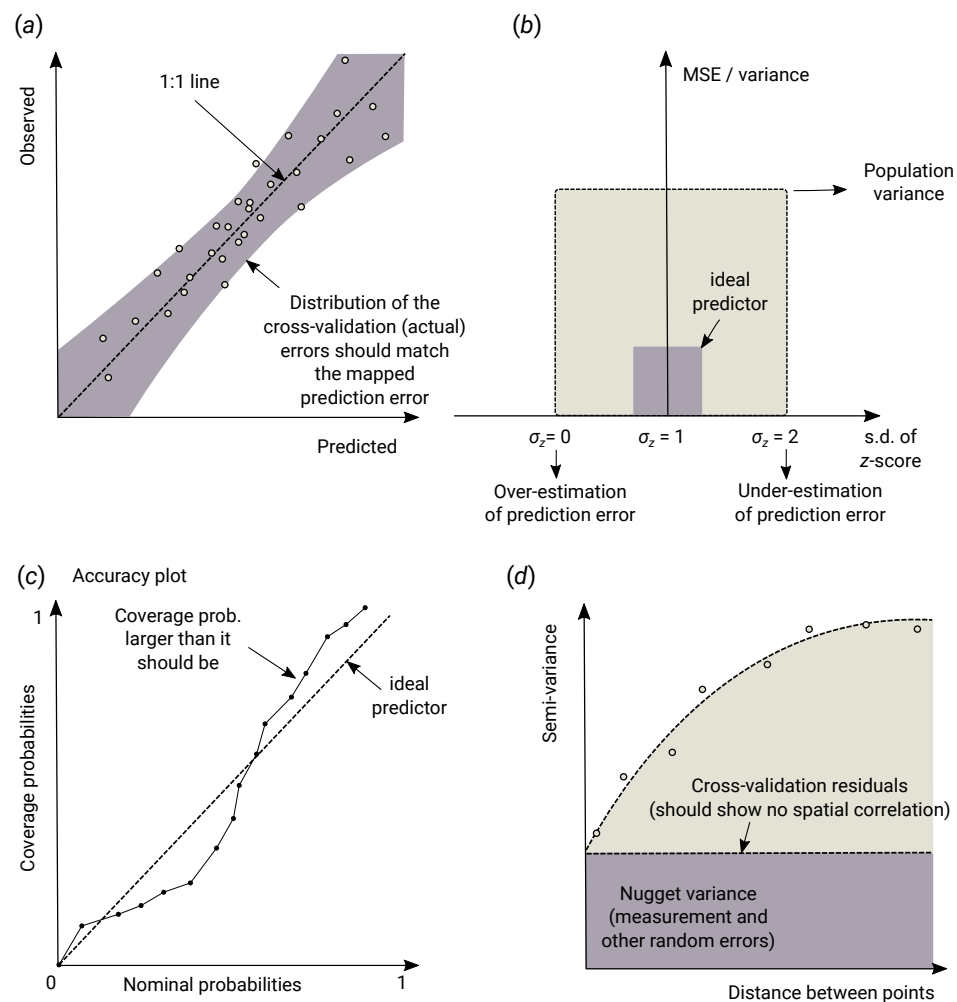


Figure 3. Schematic examples of standard mapping performance criteria used for evaluation of spatial prediction algorithms and their interpretation: (a) predicted vs. observed plot, (b) standardized accuracy vs. standard deviation of the z-scores, (c) “accuracy plots” (after Goovaerts (1999)), and (d) variogram of the target variable and the cross-validation residuals. In principle, all plots and statistics reported in this paper are based on the results of n -fold cross-validation.

$$\text{RMSE} = \sqrt{\frac{1}{m} \sum_{j=1}^m (\hat{y}(\mathbf{s}_j) - y(\mathbf{s}_j))^2}$$

$$\text{ME} = \frac{1}{m} \sum_{j=1}^m (\hat{y}(\mathbf{s}_j) - y(\mathbf{s}_j))$$

where $\hat{y}(\mathbf{s}_j)$ is the predicted value of y at cross-validation location \mathbf{s}_j , and m is the total number of cross-validation points. The amount of variation explained by the model is derived as:

$$R^2 = \left[1 - \frac{\text{SSE}}{\text{SST}} \right] \% \quad (20)$$

where SSE is the sum of squared errors at cross-validation points (i.e. $MSE \cdot n$) and SST is the total sum of squares. A coefficient of determination close to 1 indicates a perfect model, i.e., 100 % of variation has been explained by the model.

The error of estimating the variance of prediction errors can likewise be quantified via the z -score (Bivand et al., 2008):

$$z_{score}(s_j) = \frac{\hat{y}(s_j) - y(s_j)}{\sigma(s_j)} \quad (21)$$

the z -score are expected to have a mean equal to 0 and variance equal to 1. If the z -score variance is substantially smaller than 1 then the model overestimates the actual prediction uncertainty. If the z -score variance is substantially greater than 1 then the model underestimates the prediction uncertainty.

Note that, in the case of QRF, the method does not produce $\sigma(s_j)$ but quantiles of the conditional distribution. As indicated before, the variance could be computed from the quantiles. However, since this would require computation of all quantiles at a sufficiently high discretization level, prediction error standard deviation $\sigma(s_j)$ can also be estimated from the lower and upper limits of a 68.27 % prediction interval:

$$\sigma_{QRF}(s_j) \approx \frac{\hat{y}_{q=0.841}(s_j) - \hat{y}_{q=0.159}(s_j)}{2} \quad (22)$$

this however assumes that the prediction errors are symmetrical, which might not always be the case.

RESULTS

Meuse data set (regression, 2D, no covariates)

In the first example, we compare the performance of a state-of-the-art model-based geostatistical model, based on the implementation in the geoR package (Diggle and Ribeiro Jr, 2007), with the RFsp model as implemented in the ranger package (Wright and Ziegler, 2017). For this we consider the Meuse data set available in the sp package:

```
> library(sp)
> demo(meuse, echo=FALSE)
```

We focus on mapping zinc (Zn) concentrations using ordinary kriging (OK) and RFsp. To produce model and predictions using OK we use the package geoR. First, we fit the variogram model using the likfit function:

```
> library(geoR)
```

```
-----
Analysis of Geostatistical Data
For an Introduction to geoR go to http://www.leg.ufpr.br/geoR
geoR version 1.7-5.2 (built on 2016-05-02) is now loaded
-----
```

```
> zinc.geo <- as.geodata(meuse["zinc"])
> ini.v <- c(var(log1p(zinc.geo$data)),500)
> zinc.vgm <- likfit(zinc.geo, lambda=0, ini=ini.v, cov.model="exponential")
```

```
kappa not used for the exponential correlation function
-----
likfit: likelihood maximisation using the function optim.
likfit: Use control() to pass additional
      arguments for the maximisation function.
      For further details see documentation for optim.
likfit: It is highly advisable to run this function several
      times with different initial values for the parameters.
likfit: WARNING: This step can be time demanding!
-----
likfit: end of numerical maximisation.
```

300 which shows that the variogram is fitted using the maximum likelihood (ML) method, lambda=0 indicates
 301 transformation by natural logarithm (positively skewed response). Note that this is the Universal Kriging
 302 approach to modeling where transformation of the variable is set prior to variogram modeling; in the
 303 case of the RK approach, transformation is set through fitting of a GLM. Once we have estimated the
 304 variogram model, we can generate predictions, i.e., the prediction map using (Eq.13):

```
> locs <- meuse.grid@coords
> zinc.ok <- krige.conv(zinc.geo, locations=locs, krige=krige.control(obj.m=zinc.vgm))

krige.conv: model with constant mean
krige.conv: performing the Box-Cox data transformation
krige.conv: back-transforming the predicted mean and variance
krige.conv: Kriging performed using global neighbourhood
```

305 note here that geoR back-transforms the values automatically (Eq.13) preventing the user from having to
 306 find the correct unbiased back-transformation (Diggle and Ribeiro Jr, 2007), which is a recommended
 307 approach for less experienced users.

308 We compare the results of OK with geoR vs. RFsp. Since no other covariates are available, we
 309 use only geographical (buffer) distances to observation points. We first derive buffer distances for each
 310 individual point, using the buffer function in the raster package (Hijmans and van Etten, 2017):

```
> grid.dist0 <- GSIF::buffer.dist(meuse["zinc"], meuse.grid[1], as.factor(1:nrow(meuse)))
```

311 which derives a raster map for each observation point. The spatial prediction model is defined as:

```
> dn0 <- paste(names(grid.dist0), collapse="+")
> fm0 <- as.formula(paste("zinc ~ ", dn0))
```

312 i.e., in the formula zinc ~ layer.1 + layer.2 + ... + layer.155 which means that the target
 313 variable is a function of 155 covariates. Next, we overlay points and covariates to create a regression
 314 matrix, so that we can tune and fit a ranger model, and generate predictions:

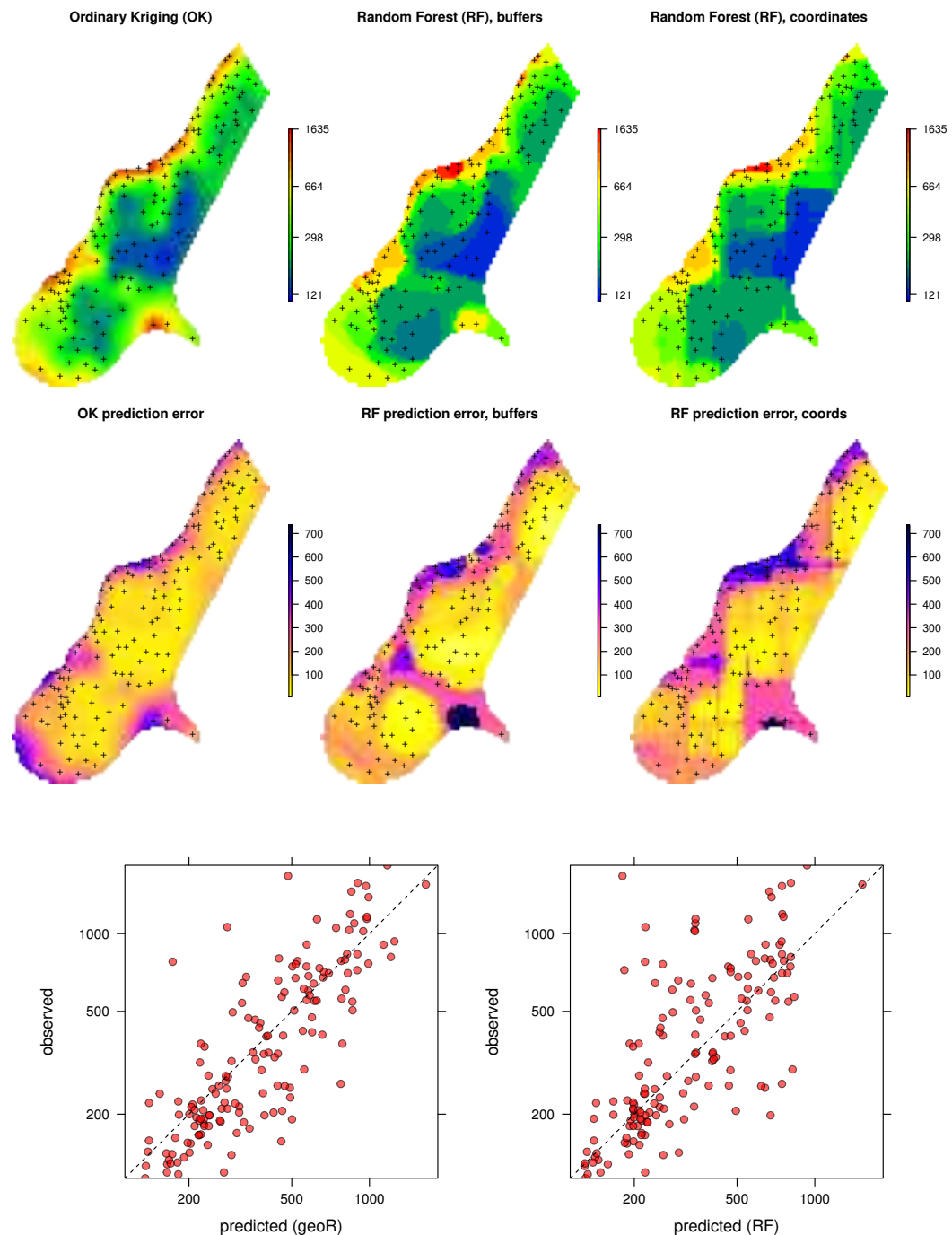


Figure 4. Comparison of predictions based on OK as implemented in the geoR package (left) and random forest (right) for zinc concentrations of the Meuse dataset: predicted concentrations in log-scale (first row), standard deviation of the prediction errors for OK and RF methods (second row, for RF based on the ranger package) and correlation plots based on the 5-fold cross-validation for OK and RFsp (last row, solid line: lowess scatterplot smoother).


```
> ov.zinc <- over(meuse["zinc"], grid.dist0)
> rm.zinc <- cbind(meuse@data["zinc"], ov.zinc)
> m.zinc <- ranger(fm0, rm.zinc, quantreg=TRUE, num.trees=150)
> m.zinc
```

Ranger result

Type:	Regression
Number of trees:	150
Sample size:	155
Number of independent variables:	155
Mtry:	98
Target node size:	4
Variable importance mode:	none
OOB prediction error (MSE):	64129.11
R squared (OOB):	0.5240641

```
> zinc.rfd <- predict(m.zinc, grid.dist0@data)
```

quantreg=TRUE allows to derive the lower and upper quantiles i.e. standard error of the predictions (Eq. 22). The out-of-bag validation R squared (OOB), indicates that the buffer distances explain about 52 % of the variation in the response.

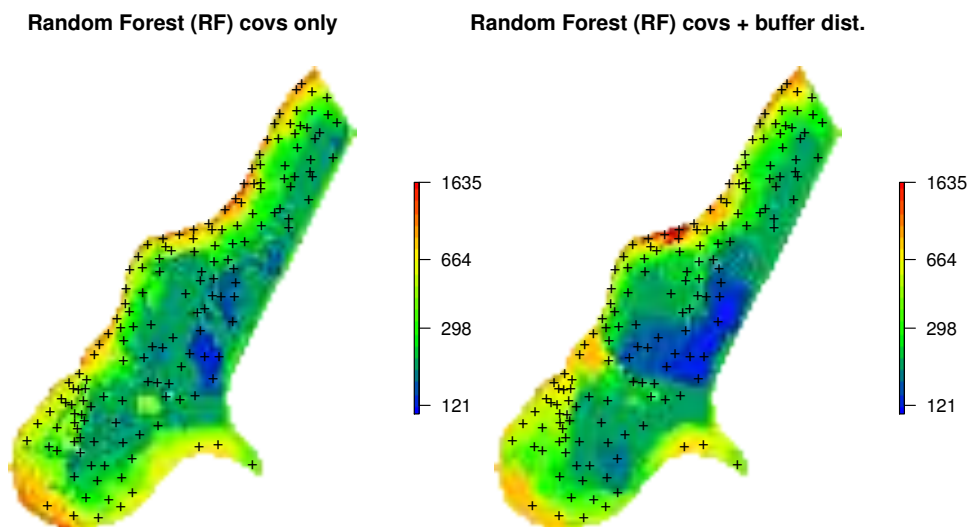


Figure 5. Comparison of predictions produced using random forest and covariates only (left), and random forest with covariates and buffer distances combined (right). Compare with Fig. 4.

Given the different approaches, the overall pattern of the spatial predictions (maps) by OK and RFsp are surprisingly similar (Fig. 4). RFsp seems to smooth the spatial pattern more than OK, which is possibly a result of the averaging of trees in random forest. Still, overall correlation between OK and RFsp maps is high ($r = 0.97$). Compared to OK, RFsp generates a more contrasting map of standard errors with clear hotspots. Note in Fig. 4, for example, how the single isolated outlier in the lower right corner is depicted by the RFsp prediction error map. Also note that, using only coordinates as predictors results in blocky artifacts (Fig. 4; right) and is probably not recommended for mapping purposes.

325 The CV results show that OK is more accurate than RFsp: R-square based on 5-fold cross-validation
326 is about 0.60 for OK and about 0.45 for RFsp. Further analysis shows that in both cases there is no
327 remaining spatial autocorrelation in the residuals (Fig. 6). Hence, both methods have fully accounted for
328 the spatial structure in the data. Both RFsp and OK seem to under-estimate the actual prediction error
329 ($\sigma(z) = 1.48$ vs. $\sigma(z) = 1.28$); in this case OK yields slightly more accurate estimates of prediction error
330 standard deviations.

331 Extension of RFsp with additional covariates means just adding further rasters to the buffer distances.
332 For example, for the Meuse data set we may add global surface water occurrence (Pekel et al., 2016) and
333 the LiDAR-based digital elevation model (DEM, <http://ahn.nl>) as potential covariates explaining
334 zinc concentration:

```
> meuse.grid$SWO <- readGDAL("Meuse_GlobalSurfaceWater_occurrence.tif")$band1[meuse.grid@grid.index]
> meuse.grid$AHN <- readGDAL("ahn.asc")$band1[meuse.grid@grid.index]
> grids.spc <- spc(meuse.grid, as.formula("~ SWO + AHN + ffreq + dist"))

Converting ffreq to indicators...
Converting covariates to principal components...
```

335 next, we fit the model using both thematic covariates and buffer distances:

```
> fm1 <- as.formula(paste("zinc ~ ", dn0, " + ", paste(names(grids.spc@predicted), collapse = "+")))
> ov.zinc1 <- over(meuse["zinc"], grids.spc@predicted)
> rm.zinc1 <- cbind(meuse@data["zinc"], ov.zinc, ov.zinc1)
> m1.zinc <- ranger(fm1, rm.zinc1, mtry=130)
m1.zinc
```

Ranger result

Type:	Regression
Number of trees:	500
Sample size:	155
Number of independent variables:	161
Mtry:	130
Target node size:	2
Variable importance mode:	impurity
OOB prediction error (MSE):	48124.16
R squared (OOB):	0.6428452

336 RFsp including additional covariates results in somewhat smaller MSE than RFsp with buffer distances
337 only. There is indeed a small difference in spatial patterns between RFsp spatial predictions derived using
338 buffer distances only (Fig. 4) and all covariates (Fig. 5): some covariates, especially flooding frequency
339 class and distance to the river, help with predicting zinc concentrations. Nevertheless, it seems that buffer
340 distances are most important for mapping zinc i.e. more important than surface water occurrence, flood
341 frequency, distance to river and elevation for producing the final predictions. This is also confirmed by
342 the variable importance table below:

```
> x1 <- as.list(ranger::importance(m1.zinc))
> print(t(data.frame(x1[order(unlist(x1), decreasing=TRUE)[1:10]])))
```

	[,1]
PC1	2171942.4
layer.54	835541.1
PC3	545576.9
layer.53	468480.8
PC2	428862.0
layer.118	424518.0
PC4	385037.8
layer.55	368511.7
layer.155	340373.8
layer.56	330771.0

which shows that, for example, points 54 and 53 are the two most influential observations, even more important than covariates (PC2–PC4) for predicting zinc concentration.

While the performance indicators show that the RFsp predictions are nearly as good as those of OK and RK, it is important to note the advantages of RFsp vs. traditional regression-kriging:

1. Spatial autocorrelation and correlation with spatial environmental factors is dealt with at once (single model in comparison with RK where regression and variogram models are often fitted separately), so that also their interactions can be modeled at once.
2. Trend model building, which is mostly done manually for kriging, is dealt with automatically in the case of RFsp. Interactions in the covariates are dealt with naturally in a tree-based method and do not need to be manually included in the linear trend as in kriging.
3. There are no 1st and 2nd order stationarity requirements (Goovaerts, 1997).
4. There is no need to fit a variogram of residuals, except to check that cross-validation residuals show no spatial autocorrelation.
5. Variable importance statistics show which individual observations and which covariates are most influential. Decomposition of R^2 as often used for linear models (Groemping, 2006) neglects model selection and does not straightforwardly apply to kriging.

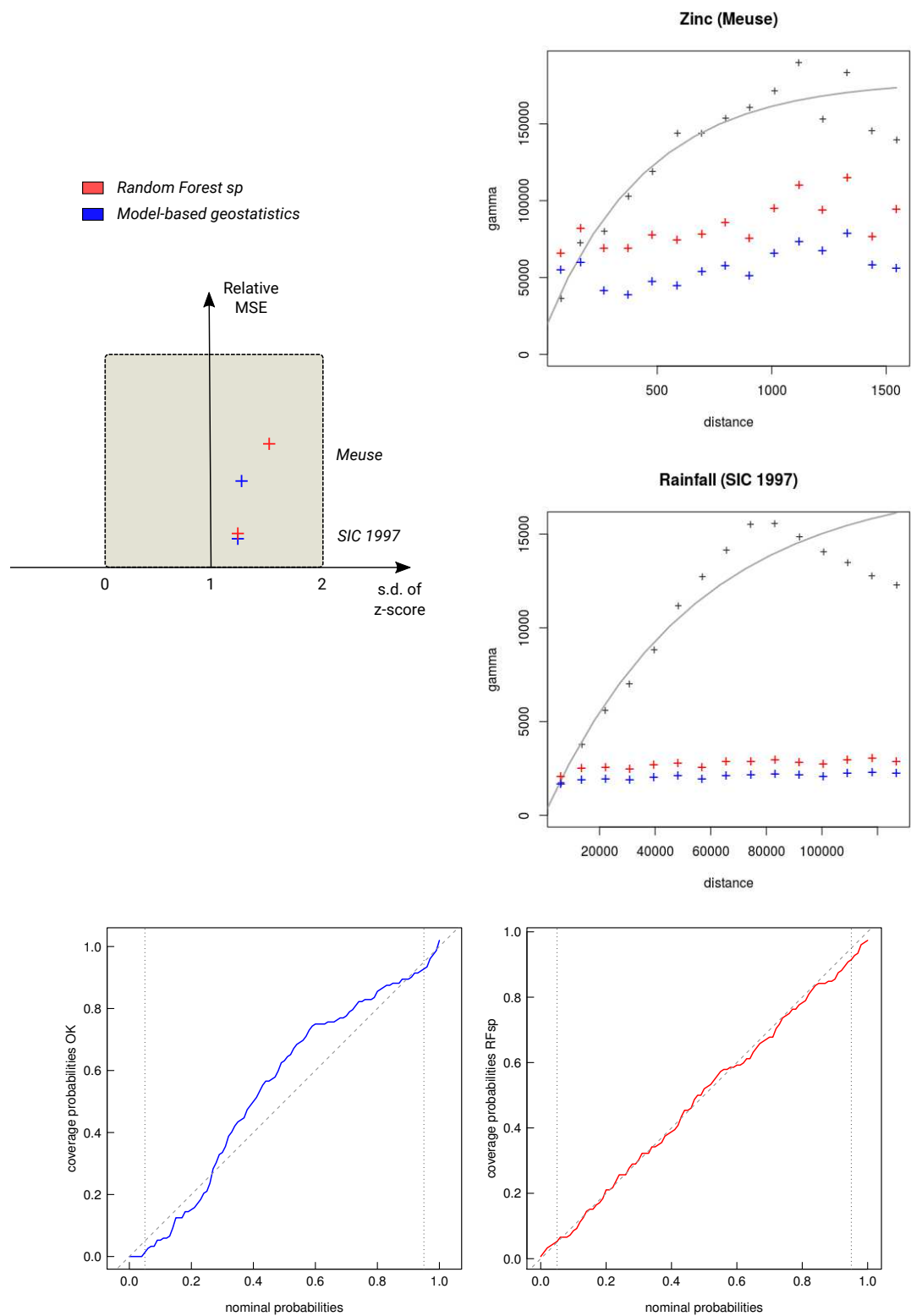


Figure 6. Summary results of cross-validation for the Meuse (zinc) and SIC 1997 (rainfall) data sets (top left) and variogram models for CV residuals (top right). Comparison of accuracy plots for the Meuse data set (below, see Fig. 3 for explanation of plots).

359 Swiss rainfall dataset data set (regression, 2D, with covariates)

360 Another interesting dataset for comparison of RFsp with linear geostatistical modeling is the Swiss rainfall
361 dataset used in the Spatial Interpolation Comparison (SIC 1997) exercise, described in detail in [Dubois](#)
362 [et al. \(2003\)](#). This dataset contains 467 measurements of daily rainfall in Switzerland on the 8th of May
363 1986. Possible covariates include elevation (DEM) and the long term mean monthly precipitation for May
364 based on the CHELSA climatic images ([Karger et al., 2017](#)) at 1 km.

365 Using geoR, we can fit an RK model:

```
> sic97.sp = readRDS("sic97.rds")
> swiss1km = readRDS("swiss1km.rds")
> ov2 = over(y=swiss1km, x=sic97.sp)
> sel.d = which(!is.na(ov2$DEM))
> sic97.geo <- as.geodata(sic97.sp[sel.d,"rainfall"])
> sic97.geo$covariate = ov2[sel.d,c("CHELSA_rainfall","DEM")]
> sic.t = ~ CHELSA_rainfall + DEM
> rain.vgm <- likfit(sic97.geo, trend = sic.t, ini=c(var(log1p(sic97.geo$data)),8000),
  fix.psiA = FALSE, fix.psiR = FALSE)

-----
likfit: likelihood maximisation using the function optim.
likfit: Use control() to pass additional
      arguments for the maximisation function.
      For further details see documentation for optim.
likfit: It is highly advisable to run this function several
      times with different initial values for the parameters.
likfit: WARNING: This step can be time demanding!
-----
likfit: end of numerical maximisation.

> rain.vgm

likfit: estimated model parameters:
      beta0      beta1      beta2      tausq      sigmasq      phi      psiA      psiR
" 166.7679" " 0.5368" " -0.0430" " 277.3047" "5338.1627" "8000.0022" " 0.7796" " 5.6204"
Practical Range with cor=0.05 for asymptotic range: 23965.86

likfit: maximised log-likelihood = -2462
```

366 where likfit is the geoR function for fitting residual variograms and:

```
sic.t = ~ CHELSA_rainfall + DEM
```

367 defines covariate variables. This produces a total of 8 model parameters including regression coefficients
368 beta, nugget and sill, anisotropy ratio and range. The rainfall data is highly anisotropic so optimizing
369 variogram modeling through likfit is important (by default, geoR implements the Restricted Maximum
370 Likelihood approach for estimation of variogram parameters, which is often considered the most reliable
371 estimate of variogram parameters; see, e.g., [Lark et al. \(2006\)](#)). The final RK predictions can be generated
372 by using the krige.conv function:

```
> locs2 = swiss1km@coords
> KC = krige.control(trend.d = sic.t,
  trend.l = ~ swiss1km$CHELSA_rainfall + swiss1km$DEM,
  obj.model = rain.vgm)
> rain.uk <- krige.conv(sic97.geo, locations=locs2, krige=KC)

krige.conv: model with mean defined by covariates provided by the user
krige.conv: anisotropy correction performed
krige.conv: Kriging performed using global neighbourhood
```

373 The results of spatial prediction using RK and RFsp are shown in Fig. 7. The cross-validation results
 374 show that in this case RFsp is nearly as accurate as RK with a cross-validation R-square of 0.78 vs. 0.82.
 375 What is striking from the Fig. 7, however, is the RFsp prediction error standard deviation map, which
 376 shows a positive correlation with the values (errors are higher in areas where rainfall values are higher),
 377 but then also depicts specific areas where it seems that the RF continuously produces higher OOB errors.
 378 The RK prediction error standard deviation map is much more homogeneous, mainly because of the
 379 stationarity assumption. This indicates that the RF prediction error map could potentially be used to
 380 depict local areas that are significantly more heterogeneous and complex and that require, either, denser
 381 sampling networks or covariates that better represent local processes in these areas.

382 The cross-validation results confirm that the prediction error standard deviations estimated by ranger
 383 and RK are both relatively similar to the actual errors. Both RFsp and RK somewhat under-estimate
 384 actual errors ($\sigma(z) = 1.16$; also visible from Fig. 7 and Fig. 6). In this case, fitting of the variogram and
 385 generation of predictions in geoR takes only a few seconds, but generation of buffer distances is more
 386 computationally intensive and is in this case the bottleneck of RFsp.

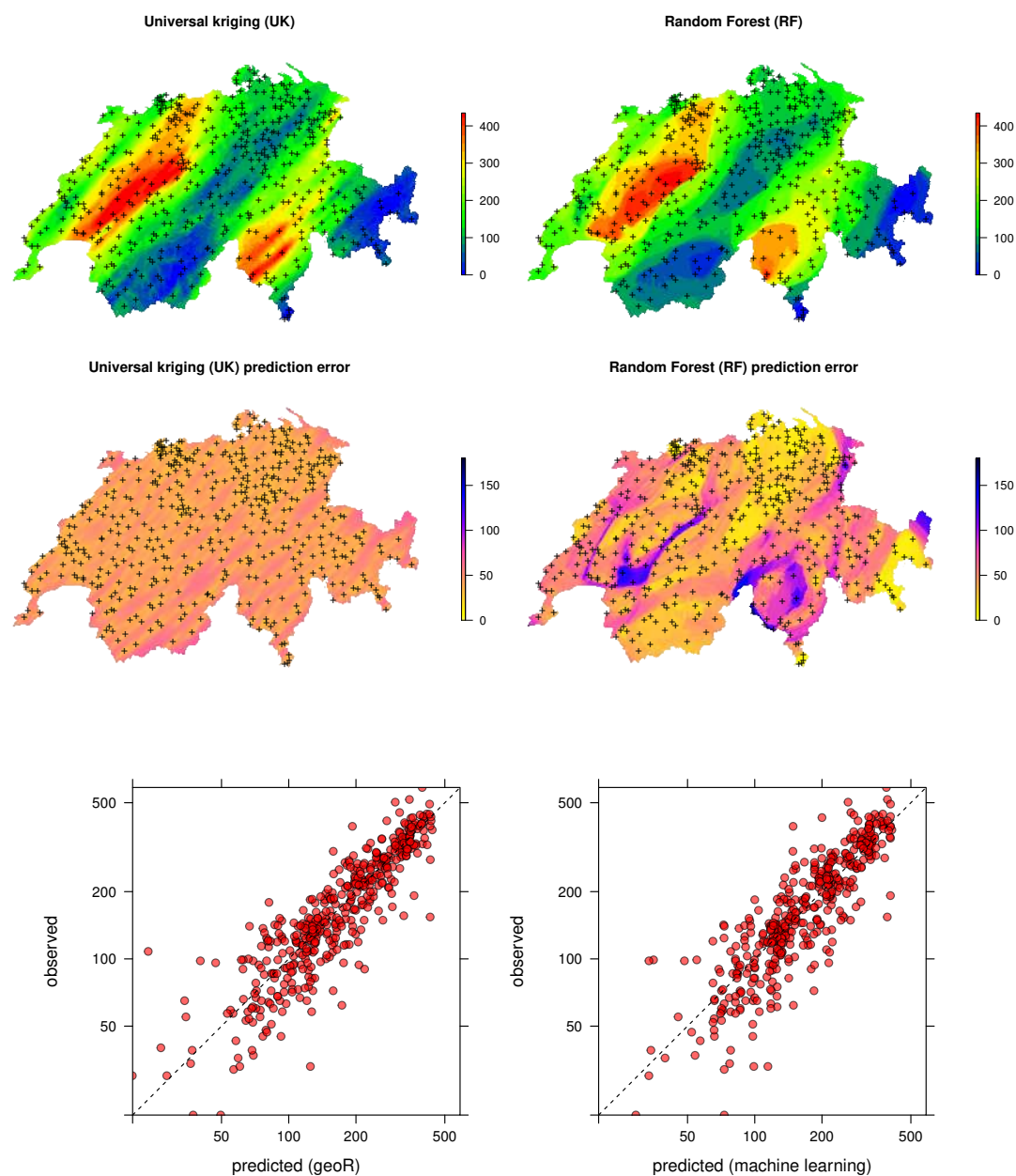


Figure 7. Comparison of predictions and standard errors produced using RK (left) and RFsp (right) for the Swiss rainfall data set (SIC 1997). Below: correlation plots based on 5-fold cross-validation. For more details about the dataset refer to [Dubois et al. \(2003\)](#).

Ebergötzen data set (binomial and multinomial variables, 2D, with covariates)

As Random Forest is a generic algorithm, it can also be used to map binomial (occurrence-type) and multinomial (factor-type) responses. These are considered to be “classification-type” problems in Machine Learning. Mostly the same algorithms can be applied as to regression-type problems, hence the R syntax is almost the same. In traditional model-based geostatistics, factor type variables can potentially be mapped using indicator kriging (Solow, 1986; Hengl et al., 2007b), but the process of fitting variograms per class, and especially for classes with few observations only, is cumbersome and unreliable.

Consider for example the Ebergötzen data set which contains 3670 ground observations of soil type, and which is one of the standard datasets used in predictive soil mapping (Böhner et al., 2006):

```
> library(plotKML)
> data(eberg)
```

We can test predicting the probability of occurrence of soil type “Parabraunerde” (according to the German soil classification; Chromic Luvisols according to the World Reference Base classification) using a list of covariates and buffer distances:

```
> eberg$Parabraunerde <- ifelse(eberg$TAXGRSC=="Parabraunerde", "TRUE", "FALSE")
> data(eberg_grid)
> coordinates(eberg) <- ~X+Y
> proj4string(eberg) <- CRS("+init=epsg:31467")
> gridded(eberg_grid) <- ~x+y
> proj4string(eberg_grid) <- CRS("+init=epsg:31467")
> eberg_spc <- spc(eberg_grid, ~ PRMGEO6+DEMSRT6+TWISRT6+TIRAST6)

Converting PRMGEO6 to indicators...
Converting covariates to principal components...

> eberg_grid@data <- cbind(eberg_grid@data, eberg_spc@predicted@data)
```

For ranger, Parabraunerde is a classification-type of problem with only two classes.

We next prepare the training data by overlaying points and covariates:

```
> ov.eberg <- over(eberg, eberg_grid)
> sel <- !is.na(ov.eberg$DEMSRT6)
> eberg.dist0 <- buffer.dist(eberg[sel,"Parabraunerde"], eberg_grid[2], as.factor(1:sum(sel)))
> ov.eberg2 <- over(eberg[sel,"Parabraunerde"], eberg.dist0)
> eb.dn0 <- paste(names(eberg.dist0), collapse="+")
> eb.fm1 <- as.formula(paste("Parabraunerde ~ ", eb.dn0, "+", paste0("PC", 1:10, collapse = "+")))
> ov.eberg3 <- over(eberg[sel,"Parabraunerde"], eberg_grid[paste0("PC", 1:10)])
> rm.eberg2 <- do.call(cbind, list(eberg@data[sel,c("Parabraunerde","TAXGRSC")], ov.eberg2, ov.eberg3))
```

so that predictions can be made from fitting the following model:

```
> eb.fm1

Parabraunerde ~ layer.1 + layer.2 + layer.3 + layer.4 + layer.5 +
...
layer.912 + PC1 + PC2 + PC3 + PC4 + PC5 + PC6 + PC7 + PC8 +
PC9 + PC10
```

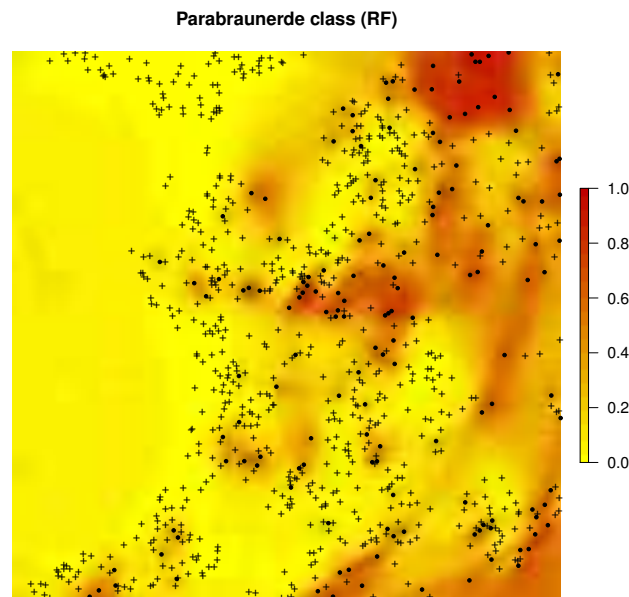



Figure 8. Predicted distribution for the Parabraunerde occurrence probabilities (the Ebergötzen data set) produced using buffer distances combined with other covariates. Dots indicate observed occurrence locations (TRUE) for the class, crosses indicate non-occurrence locations (FALSE). Predictions reveal a hybrid spatial pattern that reflects both geographical proximity (samples) and relationship between soil class and landscape (covariate or feature space).

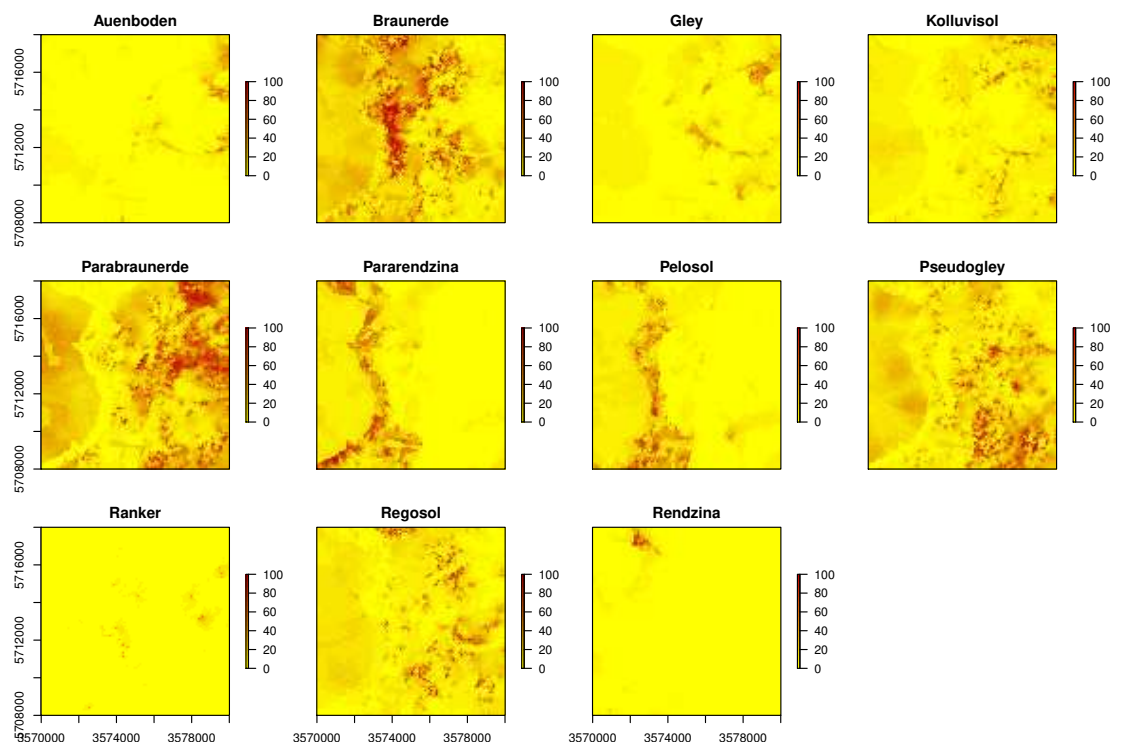


Figure 9. Predicted soil type occurrence probabilities (the Ebergötzen data set; German soil classification system) using buffer distance to each class and a stack of covariates representing parent material, hydrology and land cover.

where `layer.*` are buffer distances to each individual point, and `PC*` are principal components based on gridded covariates. This will become a hyper-parametric model as the total number of covariates exceeds the number of observations. The fitted RF model shows:

```
> m1.Parabraunerde <- ranger(eb.fm1, rm.eberg2[complete.cases(rm.eberg2),],
  importance = "impurity", probability = TRUE)
> m1.Parabraunerde

Ranger result

Type:                                Probability estimation
Number of trees:                      500
Sample size:                          829
Number of independent variables:      922
Mtry:                                 30
Target node size:                     10
Variable importance mode:             impurity
OOB prediction error:                 0.1536716
```

in this case the Out-of-Bag prediction error indicates a mean squared error of 0.15, which corresponds to a classification accuracy of >85 %. Note that we specify that we aim at deriving probabilities of the class of interest by setting `probability = TRUE`. The output map (Fig. 8) shows again a hybrid pattern: buffer distances to points have an effect at some locations, but this varies from area to area. Overall the most important covariates are PCs 1, 7, 8 and 3. Also note that binomial variable can be modeled with ranger as classification and/or regression-type (0/1 values) of problem — these are mathematically equivalent and should results in the same predictions i.e. predicted probabilities should matches regression predictions.

In a similar way we can also map all other soil types (Fig. 9). The function `GSIF::autopredict` wraps all steps described previously into a single function:

```
> soiltype <- GSIF::autopredict(eberg["TAXGRSC"], eberg_grid, auto.plot=FALSE)

Generating buffer distances...
Converting PRMGEO6 to indicators...
Converting LNCCOR6 to indicators...
Converting covariates to principal components...
Fitting a random forest model using 'ranger'...
Generating predictions...
```

in this case buffer distances are derived to each class, which is less computationally intensive than deriving distances to each individual observation locations because there are typically much fewer classes than observations. Although deriving buffer distances to each individual observation location provides certainly more detail, in the case of factor-type variables, RF might benefit well from only the distances to classes.

In summary, spatial prediction of binary and factor-type variables is straightforward with ranger, and buffer distances can be incorporated in the same way as for continuous-numerical variables. In geostatistics, handling categorical dependent variables is more complex, where the GLGM with link functions and/or indicator kriging would need to be used, among others requiring that variograms are fitted per class.

NRCS data set (weighted regression, 3D)

In many cases training data sets (points) come with variable measurement errors or have been collected with a sampling bias. If information about the data quality of each individual observation is known, then it also makes sense to use this information to produce a more balanced spatial prediction model. Package ranger allows this via the argument `case.weights` — observations with larger weights will be selected with higher probability in the bootstrap, so that the output model will be (correctly) more influenced by observations with higher weights.

Consider for example the soil point data set prepared as a combination of (a) the National Cooperative Soil Survey (NCSS) Characterization Database, and (b) National Soil Information System (NASIS) points (Ramcharan et al., 2018). The NCSS soil points contain laboratory measurements of soil clay content, while the NASIS points contain only soil texture classes determined by hand (from which also clay content can be derived), hence with much higher measurement error:

```
> carson <- read.csv(file="data/NRCS/carson_CLYPPT.csv")
> carson1km <- readRDS("data/NRCS/carson_covs1km.rds")
> coordinates(carson) <- ~ X + Y
> proj4string(carson) = carson1km@proj4string
> carson$DEPTH.f = ifelse(is.na(carson$DEPTH), 20, carson$DEPTH)
```

The number of NASIS points is much higher (ca. $5\times$) than that of the NCSS points, but the NCSS observations are about $3\times$ more accurate. We take a pragmatic approach and take the weights in the modeling procedure proportional to the quality of data:

```
> str(carson@data)

'data.frame':      3418 obs. of  8 variables:
 $ X.1      : int  1 2 3 4 5 6 8 9 10 11 ...
 $ SOURCEID : Factor w/ 3230 levels "00CA693X017jbf",...: 1392 1393 3101 3102 ...
 $ pscs     : Factor w/ 25 levels "ASHY","ASHY OVER CLAYEY",...: 19 7 16 16 16 16 7 20 20 ...
 $ CLYPPT   : int  20 64 27 27 27 27 64 20 20 ...
 $ CLYPPT.sd: int  8 16 6 6 6 6 6 16 8 8 ...
 $ SOURCEDB : Factor w/ 2 levels "NASIS","NCSS": 1 1 1 1 1 1 1 1 1 ...
 $ DEPTH    : int  NA NA NA NA NA NA NA NA NA NA ...
 $ DEPTH.f  : num  20 20 20 20 20 20 20 20 20 20 ...
```

where CLYPPT is the estimated clay fraction (m%) of the fine earth, and CLYPPT.sd is the reported measurement error standard deviation associated to each individual point (in this case soil horizon). We can build a weighted RF spatial prediction model using:

```
> rm.carson <- cbind(as.data.frame(carson), over(carson["CLYPPT"], carson1km))
> fm.clay <- as.formula(paste("CLYPPT ~ DEPTH.f + ", paste(names(carson1km), collapse = "+")))
> pars.carson <- list(num.trees=150, mtry=25, case.weights=1/(rm.carson.s$CLYPPT.sd^2))
> m.clay <- ranger(fm.clay, rm.carson, unlist(pars.carson))
```

in this case we used $1/\Delta\sigma_y^2$, i.e., inverse measurement variance as `case.weights` so that points that were measured in the lab will receive much higher weights.

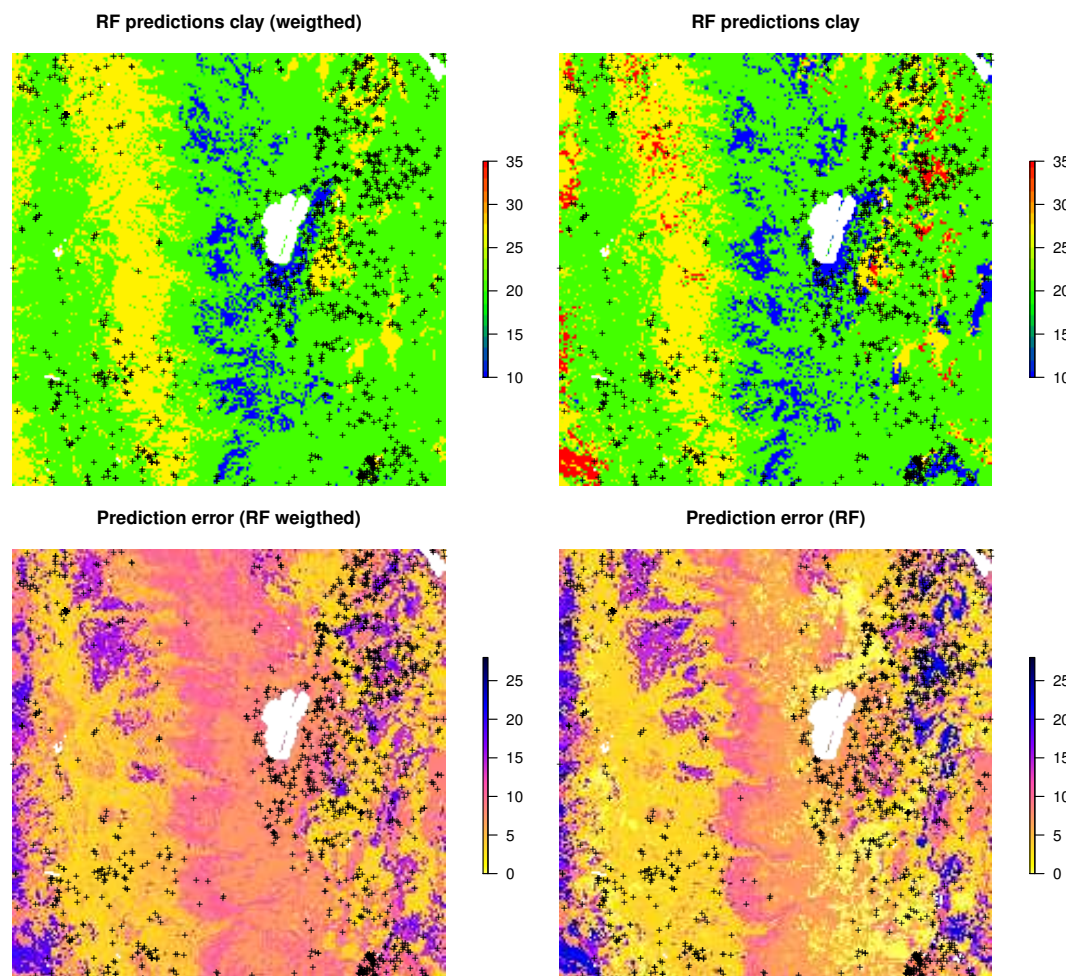


Figure 10. RF predictions and prediction error standard deviations for clay content with and without using measurement errors as weights. Study area around Lake Tahoe, California USA. Point data sources: National Cooperative Soil Survey (NCSS) Characterization Database and National Soil Information System (NASIS) (Ramcharan et al., 2018).

Fig. 10 shows that, in this specific case, the model without weights seems to predict somewhat higher values, especially in the extrapolation areas. Also the prediction error standard deviations seems to be somewhat smaller (ca. 10 %) for the unweighted regression model. This indicates that using measurement errors in model calibration is important and one should not avoid specifying this in the model, especially if the training data is heterogeneous.

The National Geochemical Survey data set, multivariate case (regression, 2D)

Because RF is a decision tree-based method, this opens a possibility to model multiple variables within a single model, i.e., by using type of variable as a covariate. This means that prediction values will show discrete jumps, depending on which variable type is used. The general form of such model is:

$$Y(s) = f \left\{ Y_{\text{type}}, C_{\text{type}}, \mathbf{X}_G, \mathbf{X}_R, \mathbf{X}_P \right\} \quad (23)$$

where Y_{type} is the variable type, i.e., chemical element, C_{type} specifies the sampling or laboratory method used, and \mathbf{X} are the covariates from Eq.(19).

Consider for example the National Geochemical Survey database that contains over 70,000 sampling points spread over the USA (Grossman et al., 2004). Here we use a subset of this dataset with 2858 points with measurements of Pb, Cu, K and Mg covering the US states Illinois and Indiana. Some useful covariates to help explain the distribution of elements in stream sediments and soils have been previously prepared (Hengl, 2009) and include:

```
> geochem <- readRDS("geochem.rds")
> usa5km <- readRDS("usa5km.rds")
> str(usa5km@data)

'data.frame':      16000 obs. of  6 variables:
 $ geomap   : Factor w/ 17 levels "6","7","8","13",...: 9 9 9 9 9 9 9 9 9 9 ...
 $ globedem : num  266 269 279 269 269 271 284 255 253 285 ...
 $ dTRI     : num  0.007 0.007 0.008 0.008 0.009 ...
 $ nlights03: num  6 5 0 5 0 1 5 13 5 5 ...
 $ dairp    : num  0.035 0.034 0.035 0.036 0.038 ...
 $ sdroads  : num  0 0 5679 0 0 ...
```

where geomap is the geological map of the USA, globedem is elevation, dTRI is the density of industrial pollutants (based on the the pan-American Environmental Atlas of pollutants), nlights03 is the lights at night image from 2003, dairp is the density of traffic based on main roads and railroads and sdroads is distance to main roads and railroads.

Since the task is to build a single model using a list of chemical elements, we need to combine all target variables into a single regression matrix. In R this can be achieved by using:

```
> geochem <- spTransform(geochem, CRS(proj4string(usa5km)))
> usa5km.spc <- spc(usa5km, ~geomap+globedem+dTRI+nlights03+dairp+sdroads)

Converting geomap to indicators...
Converting covariates to principal components...

> ov.geochem <- over(x=geochem, y=usa5km.spc@predicted)
> df.lst <- lapply(c("PB_ICP40", "CU_ICP40", "K_ICP40", "MG_ICP40"),
  function(i){cbind(geochem@data[,c(i, "TYPEDESC")], ov.geochem)})
```

Next, we rename columns that contain the target variable:

```
> t.vars = c("PB_ICP40", "CU_ICP40", "K_ICP40", "MG_ICP40")
> df.lst = lapply(t.vars, function(i){cbind(geochem@data[,c(i, "TYPEDESC")], ov.geochem)})
> names(df.lst) = t.vars
> for(i in t.vars){colnames(df.lst[[i]])[1] = "Y"}
> for(i in t.vars){df.lst[[i]]$TYPE = i}
```

so that all variables (now called Y) can be combined into a single regression matrix:

```
> rm.geochem = do.call(rbind, df.lst)
> str(rm.geochem)
```



```
'data.frame':      11432 obs. of  25 variables:
 $ Y          : num  9 10 10 9 16 14 8 15 11 9 ...
 $ TYPE       : chr  "PB_ICP40" "PB_ICP40" "PB_ICP40" "PB_ICP40" ...
 ...
```

467 where the TYPE column carries the information of the type of variable. To this regression matrix we can
468 fit a RF model of the shape:

```
> fm.g

Y ~ PC1 + PC2 + PC3 + PC4 + PC5 + PC6 + PC7 + PC8 + PC9 + PC10 +
    PC11 + PC12 + PC13 + PC14 + PC15 + PC16 + PC17 + PC18 + PC19 +
    PC20 + PC21 + TYPECU_ICP40 + TYPEK_ICP40 + TYPEMG_ICP40 +
    TYPEPB_ICP40 + TYPEDESCSOIL + TYPEDESCSTRM.SED.DRY +
    TYPEDESCSTRM.SED.WET + TYPEDESCUNKNOWN
```

469 where PC* are the principal components derived from covariates, TYPECU_ICP40 is an indicator variable
470 defining whether the variable is Cu, TYPEK_ICP40 is an indicator variable for K, TYPEDESCSOIL is
471 an indicator variable for soil sample (362 training points in total), and TYPEDESCSTRM.SED.WET is an
472 indicator variable for stream sediment sample (2233 training points in total).

473 The RF fitted to these data gives:

```
> rm.geochem.e <- rm.geochem.e[complete.cases(rm.geochem.e),]
> m1.geochem <- ranger(fm.g, rm.geochem.e, importance = "impurity")
> m1.geochem
```

Ranger result

Type:	Regression
Number of trees:	500
Sample size:	11148
Number of independent variables:	29
Mtry:	5
Target node size:	5
Variable importance mode:	impurity
OOB prediction error (MSE):	1462.767
R squared (OOB):	0.3975704

474 To predict values and generate maps we need to specify (a) type of chemical element, and (b) type of
475 sampling medium at the new predictions locations:

```
> new.usa5km = usa5km.spc@predicted@data
> new.usa5km$TYPEDESCSOIL = 0
> new.usa5km$TYPEDESCSTRM.SED.DRY = 0
> new.usa5km$TYPEDESCSTRM.SED.WET = 1
> new.usa5km$TYPEDESCUNKNOWN = 0
> for(i in t.vars){
  new.usa5km[,paste0("TYPE",i)] = 1
  for(j in t.vars[!t.vars %in% i]){ new.usa5km[,paste0("TYPE",j)] = 0 }
  x <- predict(m1.geochem, new.usa5km)
  usa5km@data[,paste0(i,"_rf")] = x$predictions
}
```

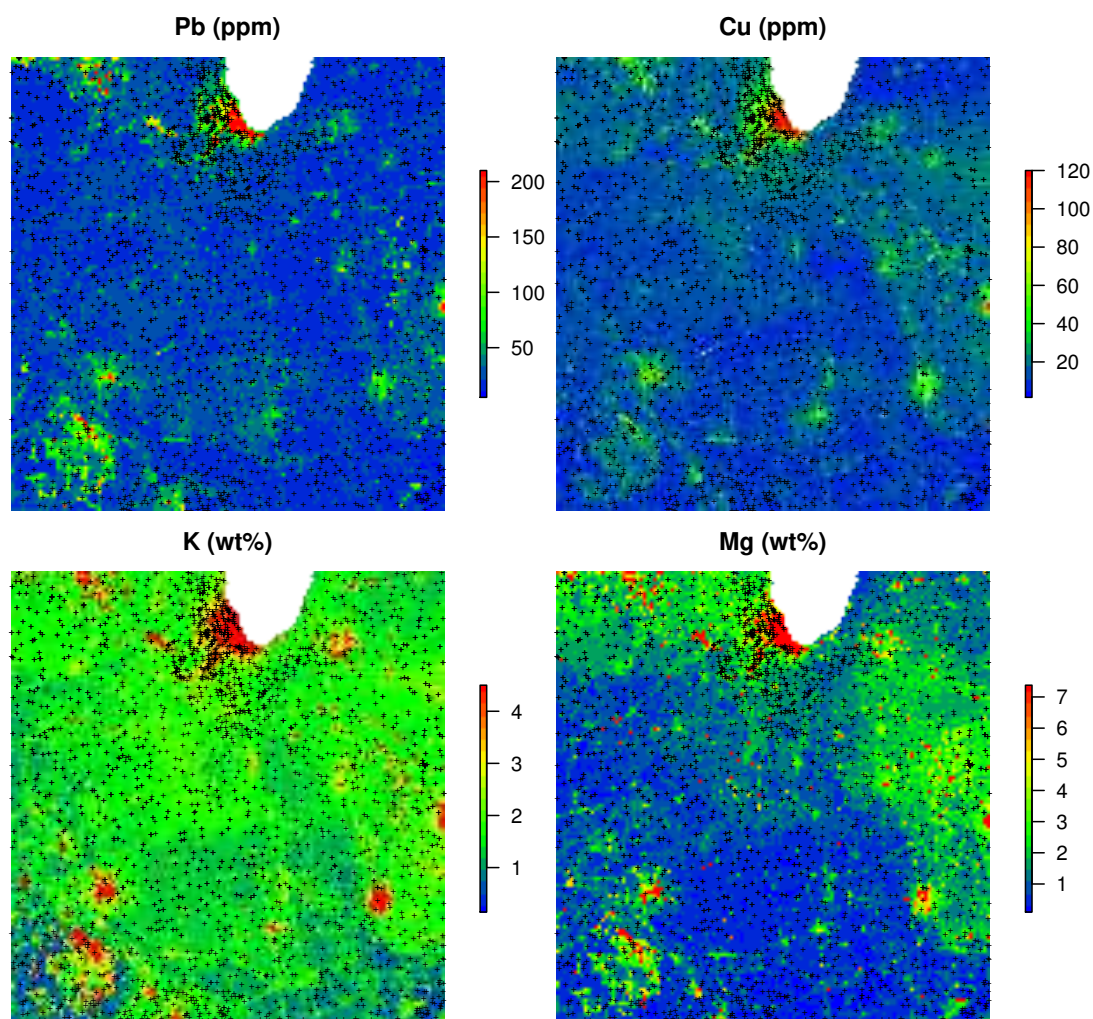


Figure 11. Predictions produced for four chemical elements (wet stream sediments) from the National Geochemical Survey using a single multivariate RF model. The study area covers the US States Illinois and Indiana. The spatial resolution of predictions is 5 km. Crosses indicate sampling locations.

476 The results of the prediction are shown in Fig. 11. From the produced maps, we can see that the spatial
 477 patterns of the four elements are relatively independent (apart from Pb and Cu which seem to be highly
 478 cross-correlated), even though they are based on a single RF model. Note also that, just by switching the
 479 TYPEDES we could produce predictions for a variety of combinations of sampling conditions and chemical
 480 elements.

481 A disadvantage of running multivariate models is that the data size increases rapidly and hence also
 482 the computing intensity. For a comparison, the National Geochemical Survey comprises hundreds of
 483 chemical elements hence the total size of training points could easily exceed several millions. In addition,
 484 computation of model diagnostics such as variable importance becomes difficult as all variables are
 485 included in a single model — ranger indicates an overall R-square of 0.40, but not all chemical elements
 486 can be mapped with the same accuracy. On the other hand, it appears that extension from univariate to
 487 multivariate spatial predictions models is fairly straightforward and can be compared to various co-kriging
 488 techniques used in the traditional geostatistics (Pebesma, 2004).

Daily precipitation Boulder (CO) data set (regression, 2D+T)

In the last example we look at extending 2D regression based on RFsp to spatiotemporal data, i.e., to a 2D+T case. For this we use a time series of daily precipitation measurements obtained from <https://www.ncdc.noaa.gov> for the period 2014–2017 for the area around Boulder Colorado:

```
> co_prec = readRDS("data/st_prec/boulder_prcp.rds")
> str(co_prec)

'data.frame':      176467 obs. of  16 variables:
 $ STATION  : Factor w/ 239 levels "US1COB00004",...: 64 64 64 64 64 64 64 64 64 64 ...
 $ NAME     : Factor w/ 233 levels "ALLENS PARK 1.5 ESE, CO US",...: 96 96 96 96 96 96 96 96 96 96 ...
 $ LATITUDE : num  40.1 40.1 40.1 40.1 40.1 ...
 $ LONGITUDE: num  -105 -105 -105 -105 -105 ...
 $ ELEVATION: num  1567 1567 1567 1567 1567 ...
 $ DATE     : Factor w/ 1462 levels "2014-11-01","2014-11-02",...: 7 13 21 35 46 67 68 69 70 75 ...
 $ PRCP     : num  0 0.16 0 0 0 0.01 0.02 0.02 0.02 0.01 ...

> co_locs.sp = co_prec[!duplicated(co_prec$STATION),c("STATION", "LATITUDE", "LONGITUDE")]
> coordinates(co_locs.sp) = ~ LONGITUDE + LATITUDE
> proj4string(co_locs.sp) = CRS("+proj=longlat +datum=WGS84")
```

Even though the monitoring network consists of only 225 stations, the total number of observations exceeds 170,000. Note also that daily precipitation is a zero-inflated variable, hence modeling it using standard model-based geostatistics is difficult (Hengl et al., 2010).

To represent ‘distance’ in the time domain, we use two numeric variables — cumulative days since 1970 and Day of the Year (DOY):

```
> co_prec$cdate = floor(unclass(as.POSIXct(as.POSIXct(paste(co_prec$DATE), format="%Y-%m-%d")))/86400)
> co_prec$doy = as.integer(strftime(as.POSIXct(paste(co_prec$DATE), format="%Y-%m-%d"), format = "%j"))
```

variable `doy` is important to represent seasonality effects while cumulative days are important to represent long term trends. We can now prepare a spatiotemporal regression matrix by combining geographical covariates, including time and additional covariates available for the area (elevation map and the long-term precipitation map based on the PRISM project <http://www.prism.oregonstate.edu/normals/>):

```
> co_grids <- readRDS("data/st_prec/boulder_grids.rds")
> co_grids <- as(co_grids, "SpatialPixelsDataFrame")
> co_locs.sp <- spTransform(co_locs.sp, co_grids@proj4string)
> sel.co <- over(co_locs.sp, co_grids[1])
> co_locs.sp <- co_locs.sp[!is.na(sel.co$elev_1km),]
> grid.distP <- GSIF::buffer.dist(co_locs.sp["STATION"], co_grids[1], as.factor(1:nrow(co_locs.sp)))
> ov.lst <- list(co_locs.sp@data, over(co_locs.sp, grid.distP), over(co_locs.sp, co_grids))
> ov.prec <- do.call(cbind, ov.lst)
> rm.prec <- plyr::join(co_prec, ov.prec)

Joining by: STATION

> rm.prec <- rm.prec[complete.cases(rm.prec[,c("PRCP", "elev_1km", "cdate")]),]
```

Next, we define a spatiotemporal model as:

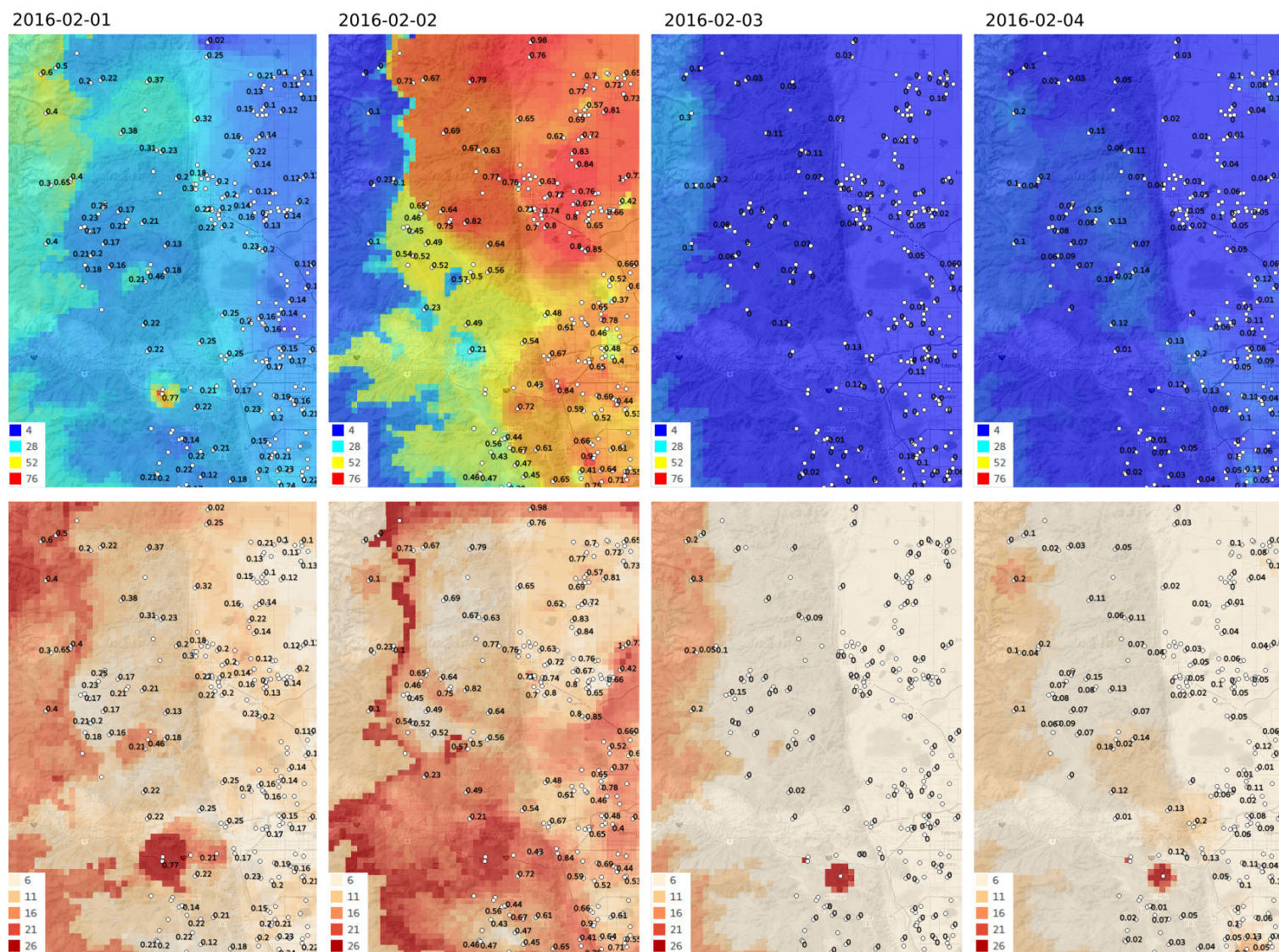


Figure 12. Spatiotemporal observations (points) and predictions of daily rainfall in mm for four days in February using the RFsp method: (above) predictions, (below) prediction error standard deviations estimated using the ranger package.

```
> fmP <- as.formula(paste("PRCP ~ cdate + doy + elev_1km + PRISM_prec +", dnP))
```

503 In other words, daily precipitation is modeled as a function of the cumulative day, day of the year,
504 elevation, long-term annual precipitation pattern and geographical distances to stations. Further modeling
505 of the spatiotemporal RFsp is done the same way as with the 2D models:

```
> m1.prec <- ranger(fmP, rm.prec, importance = "impurity", num.trees = 150, mtry = 180)
> m1.prec
```

Ranger result

Type:	Regression
Number of trees:	150
Sample size:	157870
Number of independent variables:	229
Mtry:	180
Target node size:	5
Variable importance mode:	impurity
OOB prediction error (MSE):	0.0052395
R squared (OOB):	0.8511794

```
> x1P.g <- as.list(m1.prec$variable.importance)
> print(t(data.frame(x1P.g[order(unlist(x1P.g), decreasing=TRUE)[1:10]])))
```

	[,1]
cdate	93.736193
doy	87.087606
PRISM_prec	2.604196
elev_1km	2.568251
layer.145	2.029082
layer.219	1.718599
layer.195	1.531632
layer.208	1.517833
layer.88	1.510936
layer.90	1.396900

506 The results indicate that clearly the most important covariate for predicting daily precipitation from this
507 study area is: time i.e. cumulative and/or day of the year. Note that, because 1–2 covariates dominate the
508 model, it is also important to keep mtry high (e.g. $> p/2$ where p is the number of independent variables),
509 because a standard value for mtry could result in time being systematically missed from selection and
510 hence in a very poor fit.

511 The single spatiotemporal model can now be used to predict anywhere within the spacetime domain,
512 which typically means producing time series of rasters contains predictions for a series of days (Fig. 12).
513 Note from Fig. 12 that some hot spots in the prediction error maps from previous days might propagate to
514 other days, which indicates spatiotemporal connection between values. This shows that RFsp connects
515 space and time in a similar way as the model-based geostatistics.

DISCUSSION

Summary results

We have defined a RFsp framework for spatial and spatiotemporal prediction of sampled variables as a data-driven modeling approach that uses three groups of covariates inside a single method:

1. geographical proximity to and composition of the sampling locations,
2. covariates describing past and current physical, chemical and biological processes,
3. spectral reflectances as direct observation of surface or sub-surface characteristics.

We have tested the RFsp framework on real data. Our tests indicate that RFsp often produces similar predictions as OK and/or RK and does so consistently, i.e., proven through repeated case studies with diverse distributions and properties of the target variable. In the case of zinc prediction for the Meuse data set, the accuracy for RFsp is somewhat smaller than for OK (Fig. 6). In this case, RFsp with buffer distances as the only covariates evidently smoothed out predictions more distinctly than kriging. As the data size increases and as more covariate layers are added, RFsp often leads to satisfactory RMSE and ME at validation points, while showing no spatial autocorrelation in the cross-validation residuals (Fig. 6). This makes RFsp interesting as a generic predictor for spatial and spatiotemporal data, comparable to state-of-the-art geostatistical techniques already available in the packages gstat and/or geoR.

Random forest has several advantages over kriging:

- There is no need to define an initial variogram, nor to fit a variogram,
- There is no need to define a search radius for kriging,
- There is no need to specify a transformation of the target variable or do any back-transformation,
- There is no need to deal with all interactions and non-linearities.

Hence, in essence, random forest requires much less expert knowledge, which has its advantages but also disadvantages as the system can appear to be a black-box without a chance to save outputs that could be result of artifacts in the data. Other obvious advantages of using random forests are:

- Information overlap (multicollinearity) and over-parameterization, caused by using too many covariates, is not a problem for RFsp. In the first example we used 155 covariates to model with 155 points, and this did not lead to biased estimation because RF has built-in protections against overfitting. RF can be used to fit models with large number of covariates, even more covariates than observations can be used.
- Sub-setting of covariates is mostly not necessary; in the case of model-based geostatistics, over-parameterization and/or overlap in covariates is a more serious problem as it can lead to biased predictions.
- RF is resistant to noise (Strobl et al., 2007).

- Geographical distances can be extended to more complex distances such as watershed distance along slope lines and or visibility indices, as indicated in the Fig. 2.

Some important drawbacks of RF, on the other hand, are:

- Predicting values using RF beyond the range in the training data is not recommended as it can lead to even poorer results than if simple linear models are used.
- RF will lead to biased predictions when trained with data sets that are sampled in a biased way (Strobl et al., 2007).
- Size of the produced models is much larger than for linear models, hence the output objects are large.
- Estimating RF model parameters and predictions is computationally intensive.
- Derivation of buffer distances is computationally intensive and storage demanding.

We do not recommend using buffer distances as covariates with RFsp for a large number of training points e.g. $\gg 1000$ since the number of maps that need to be produced could blow up the production costs, and also computational complexity of such models would become cumbersome.

On the other hand, because exceptionally simple neural networks can be used to represent inherently complex ecological systems, and because computing costs are exponentially decreasing, it can be said that most of the generic Machine Learning techniques are in fact ‘cheap’ and have quickly become mainstream data science methods (Lin et al., 2017). Also, we have shown that buffer distances do not have to be derived to every single observation point — for factors it turned out that deriving distances per class worked quite well. For numeric variables, values can be split into 10–15 classes (from low to high) and then again distances can be only derived to low and high values. In addition, limiting the number and complexity of trees in the random forest models (Latinne et al., 2001), e.g., from 500 to 80 often leads to minimum losses in accuracy, so there is certainly room for reducing size and complexity of ML models without significantly loosing on accuracy.

Is there still need for kriging?

Given the comparison results we have shown previously, we can justifiably ask whether there is still a need for model-based geostatistics at all? Surely, fitting of spatial autocorrelation functions, i.e., variograms will remain a valuable tool, but it does appear from the examples above that RFsp is more generic and more flexible for automation of spatial predictions than any version of kriging. This does not mean that students should not bother with learning principles of kriging and geostatistics. In fact, with RFsp we need to know geostatistics more than ever, as these tools will enable us to generate more and more analyses, and hence we will also need to boost our interpretation skills. So, in short, kriging as a spatial prediction technique might be redundant, but solid knowledge of geostatistics and statistics in general is important more than ever. Also with RFsp, we still needed to fit variograms for cross-validation residuals and derive occurrence probabilities etc. All this would have been impossible without understanding principles of spatial statistics, i.e., geostatistics.

While we emphasize that data-driven approaches such as RF are flexible and relatively easy to use because they need not go through a cumbersome procedure of defining and calibrating a valid geostatistical model, we should also acknowledge the limitations of data-driven approaches. Because there is no model one can also not inspect and interpret the calibrated model. Parameter estimation becomes essentially a heuristic procedure that cannot be optimized, other than through cross-validation. Finally, extrapolation with data-driven methods is more risky than with model-based approaches, in fact serious extrapolation with RF models is not recommended at all.

Are geographic covariates needed at all?

The algorithm that is based on deriving buffer distance maps from observation points is not only computationally intensive, it also results in a large number of maps. One can easily imagine that this approach would not be ready for operational use where $\gg 1000$ as the resources needed to do any analysis would simply blow up. But are buffer distances needed at all? Can the geographical location and proximity of points be included in the modeling using something less computationally intensive?

McBratney et al. (2003) have, for example, conceptualized the so-called “*scorpan*” model in which soil property is modeled as a function of:

- (auxiliary) soil properties,
- climate,
- organisms, vegetation or fauna or human activity,
- relief,
- parent material,
- age i.e. the time factor,
- n space, spatial position,

It appears that also s and n could be represented as a function of other environmental gradients. In fact, it can be easily shown that, as long as there are enough unique covariates available that explain the majority of physical and chemical processes (past and current) and enough remote sensing data that provides spectral information about the object / feature, each point on the Globe can be defined with an unique ‘signature’, so that there is probably no need for including spatial location in the predictive mapping at all.

In other words, as long as we are able to prepare, for example, hundreds of covariates that explain in detail uniqueness of each location (or as long an algorithm can not find many duplicate locations with unique signature), and as long as there are enough training point to describe spatial relations, there is probably no need to derive buffer distances to all points at all. In the example by Ramcharan et al. (2018), almost 400,000 points and over 300 covariates are used for training a MLA-based prediction system: strikingly the predicted maps show kriging-like pattern with spatial proximity to points included, even though no buffer distances were ever derived and used. It appears that any tree-based machine learning

system that can ‘learn’ about the uniqueness of a geographical location will eventually be able to represent geographical proximity also in the predictions. What might be still useful is to select a smaller subset of points where hot-spots or points with high CV error appear, then derive buffer distances only to those points and add them to the bulk of covariates.

Behrens et al. (2018) have recently discovered that, for example, DEM derivatives correlate derived at coarser scales correlate more with some targeted soil properties than the derivatives derived as fine scales; in this case, scale was represented through various DEM aggregation levels and filter sizes. Some physical and chemical processes of soil formation or vegetation distribution might not be visible at finer aggregation levels, but then become very visible at coarser aggregation levels. In fact, it seems that spatial dependencies and interactions of the covariates can be explained simply by aggregating DEM and the derivatives. For long time physical geographers have imagined that climate, vegetation and similar are non-linear function of longitude and latitude; now appears also that vice versa could be also valid.

Remaining methodological problems and future directions

Even though MLA has proven to be efficient in boosting spatial prediction performance, there still remain several methodological problems before it can be widely applied, for example:

- How to generate spatial simulations that accurately represents spatial autocorrelation structure using RF models?
- How to produce predictions at various block support sizes — from point support data to block support data and vice versa?
- How to account for spatial and spatiotemporal clustering of points?

Meyer et al. (2018) have recently shown that, if repeated spatial observations exist or observations that are linked to the same location, that RF will also use that knowledge in the training process, which will then lead to some covariates becoming ‘artificially’ more important than they should be. Consequently, the overall accuracy estimated by ranger using Out-of-Bag samples becomes over-optimistic. In our spatio-temporal data, for example, we have ignored the fact that meteo stations have fixed locations, but in practice Meyer et al. (2018) have shown that this has serious effects on model training. To get a more realistic measure of the mapping accuracy, cross-validation techniques such as the Leave-Location-Out, as implemented in the mlr package (Bischl et al., 2016) or similar, would be thus be a better choice for this purpose.

Although Machine Learning is often very successful in spatial prediction, we should not be over-relaxed by its flexibility and efficiency of crunching data. Any purely data or pattern driven classifier or regressor is a rather mechanical approach to problem solving. It ignores all of our knowledge of processes and relationships that have been documented and proven to work over and over. It does not have an explicit (geo)statistical model as a starting point, so that no mathematical derivations are possible at all. Also, just adding more and more data to the system does not necessarily mean that the predictions will automatically become better (Zhu et al., 2012). In that context, what seems a logical direction for Machine Learning is development of hybrid use of data and model, i.e., an A.I. systems that not only mechanically

mines data, but also mines models and knowledge and extends from testing accuracy improvements to testing more complex measures of modeling success such as model simplicity, importance of models across various domains of science (even testing mathematical proofs?). Such model would have been at the order of magnitude more complex than Machine Learning, but, given the exponential growth of the field of A.I., this might not take decades to achieve.

One model to rule them all

Given that with RF multiple variables can be predicted at once, and given that all global data from some theme such as soil science, meteorology etc, could be put into a single harmonized and integrated database, one could argue that, in the near future, a single machine learning model could be fitted to explain all spatial and/or spatio-temporal patterns within some domain of science such as soil science, meteorology, biodiversity etc. This is assuming that ALL observations and measurements within that domain have been integrated and pre-processed / harmonized for use. Such models could potentially be used as '*knowledge engines*' for various scientific fields, and could be served on-demand, i.e., they would generate predictions only if the predictions are required by the users.

These data set and models would be increasingly large. In fact, they would probably require super computing power to update them and a high capacity network to serve them, hence the current state-of-the-art data science might gradually move from managing Big Data only, to managing Big Data and Big Models.

CONCLUSIONS

We have shown that random forest can be used to generate unbiased spatial predictions and model and map uncertainty. Through several standard textbook datasets, we have shown that the predictions produced using RFsp are often equally accurate (based on repeated cross-validation) than equivalent linear geostatistical models. The advantages of random forest vs. linear geostatistical modeling and techniques such as kriging, however, lies in the fact that no stationarity assumptions need to be followed, nor is there a need to specify transformation or anisotropy parameters (or to fit variograms at all!).

This makes RF fairly attractive for automated mapping applications, especially where the point sampling is representative (extrapolation minimized) and where relationship between the target variable, covariates and spatial dependence structure is complex, non-linear and requires localized solutions. Some serious disadvantage of using RFsp, on the other hand, is sensitivity to input data quality, extrapolation problems. For RFsp also training data quality is the key to success, hence ideally samples collected using objective sampling designs, careful cleaning of data, and exclusion of uncontrolled factors is highly recommended. Spatial clustering or sampling bias, typos in the data or mismatches in coordinates can result in non-nonsensical outputs, without the mapper even being aware of it.

Based on discussion above, we can recommend a two-stage framework explained in Fig. 13, as possibly the shortest path to generating maximum mapping accuracy whilst saving the production costs. In the first stage, initial samples are used to get an estimate of the model parameters, this initial information is then used to optimize predictions (the second stage) so that the mapping objectives can be achieved with minimum additional investments. The framework in Fig. 13, however, assumes that there are

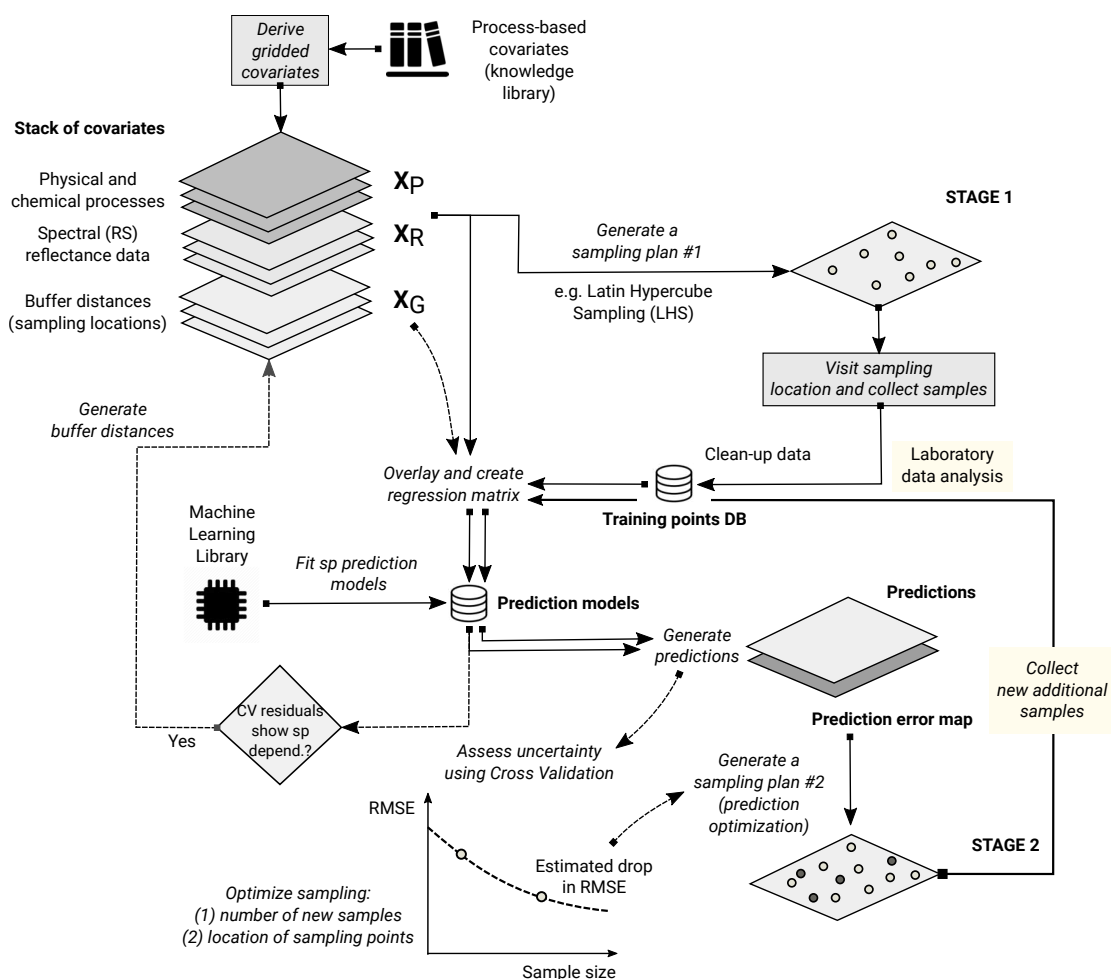


Figure 13. The recommended two-stage accuracy-driven framework for optimizing spatial predictions based on RFsp (see also Eq. 19). In the first stage, minimum number of objectively sampled points are used to get an initial estimate of the model. In the second stage, the exact number of samples and sampling locations are allocated using the prediction error map, so that the mapping accuracy can be brought towards the desired or target confidence intervals.

(just) enough objectively sampled initial samples, that the RF error map is reliable, i.e., accurate, that robust cross-validation is used and a reliable RMSE decay function. Simple decay functions could be further extended to include also objective ‘cooling’ functions as used for example in Brus and Heuvelink (2007), although these could likely blow-up computational intensity. Two-stage sampling is already quite known in literature (Hsiao et al., 2000; Meerschman et al., 2011; Knotters and Brus, 2013), and further optimization and automation of two-stage sampling would possibly be quite interesting to reduce mapping costs.

Even though we have provided comprehensive guidelines on how to implement RF for various predictive mapping problems — from continuous to factor-type variables and from purely spatial to spatiotemporal problems with multiple covariates — there are also still many methodological challenges, such as derivation of spatial simulations, derivation of buffer distances for large point data sets etc, to be solved before RFsp can become fully operational for predictive mapping.

ACKNOWLEDGMENTS

We are grateful to the developers of the original random forest algorithms (Breiman, 2001), Philipp Probst for developing algorithms for fine-tuning of RF and implementing the Quantile Regression Forests, and the developers of the spatial analysis packages GDAL, rgdal, raster, sp (Pebesma, 2004; Bivand et al., 2008), and SAGA GIS (Conrad et al., 2015), on top of which we have built work-flows and examples of applications.

REFERENCES

- Behrens, T., Schmidt, K., MacMillan, R., and Rossel, R. V. (2018). Multiscale contextual spatial modelling with the gaussian scale space. *Geoderma*, 310:128 – 137.
- Biau, G. and Scornet, E. (2016). A random forest guided tour. *TEST*, 25(2):197–227.
- Bischl, B., Lang, M., Kotthoff, L., Schiffner, J., Richter, J., Studerus, E., Casalicchio, G., and Jones, Z. M. (2016). mlr: Machine learning in R. *Journal of Machine Learning Research*, 17(170):1–5.
- Bivand, R. S., Pebesma, E. J., Gomez-Rubio, V., and Pebesma, E. J. (2008). *Applied Spatial Data Analysis with R*, volume 747248717. Springer.
- Böhner, J., McCloy, K., and Strobl, J. (2006). Saga—analysis and modelling applications, vol. 115. *Göttinger Geographische Abhandlungen, Göttingen*, 130.
- Boulesteix, A.-L., Janitza, S., Kruppa, J., and König, I. R. (2012). Overview of random forest methodology and practical guidance with emphasis on computational biology and bioinformatics. *Wiley Interdisciplinary Reviews: Data Mining and Knowledge Discovery*, 2(6):493–507.
- Breiman, L. (2001). Random forests. *Machine Learning*, 45(1):5–32.
- Brown, P. E. (2015). Model-based geostatistics the easy way. *Journal of Statistical Software*, 63(12).
- Brus, D. J. and Heuvelink, G. B. (2007). Optimization of sample patterns for universal kriging of environmental variables. *Geoderma*, 138(1):86–95.
- Christensen, R. (2001). *Linear Models for Multivariate, Time Series, and Spatial Data*. Springer Verlag, New York, 2nd edition.
- Conrad, O., Bechtel, B., Bock, M., Dietrich, H., Fischer, E., Gerlitz, L., Wehberg, J., Wichmann, V., and Böhner, J. (2015). System for automated geoscientific analyses (saga) v. 2.1. 4. *Geoscientific Model Development*, 8(7):1991–2007.
- Coulston, J. W., Blinn, C. E., Thomas, V. A., and Wynne, R. H. (2016). Approximating prediction uncertainty for random forest regression models. *Photogrammetric Engineering & Remote Sensing*, 82(3):189 – 197.
- Cressie, N. (1990). The origins of kriging. *Mathematical Geology*, 22(3):239–252.
- Cressie, N. (2015). *Statistics for Spatial Data*. Wiley Series in Probability and Statistics. Wiley.
- Cutler, D. R., Edwards, T. C., Beard, K. H., Cutler, A., Hess, K. T., Gibson, J., and Lawler, J. J. (2007). Random forests for classification in ecology. *Ecology*, 88(11):2783–2792.
- Deutsch, C. V. and Journel, A. G. (1998). *Geostatistical Software Library and User's Guide*. Oxford University Press, New York.
- Diggle, P. J. and Ribeiro Jr, P. J. (2007). *Model-based Geostatistics*. Springer Series in Statistics. Springer.

- 745 Dubois, G., editor (2005). *Automatic Mapping Algorithms for Routine and Emergency Monitoring Data*.
746 Report on the Spatial Interpolation Comparison (SIC2004) exercise. EUR 21595 EN. Office for Official
747 Publications of the European Communities, Luxembourg.
- 748 Dubois, G., Malczewski, J., and De Cort, M. (2003). *Mapping Radioactivity in the Environment: Spatial*
749 *Interpolation Comparison 97*. EUR 20667 EN. Office for Official Publications of the European
750 Communities.
- 751 Goldberger, A. (1962). Best Linear Unbiased Prediction in the Generalized Linear Regression Model.
752 *Journal of the American Statistical Association*, 57:369–375.
- 753 Goovaerts, P. (1997). *Geostatistics for Natural Resources Evaluation (Applied Geostatistics)*. Oxford
754 University Press, New York.
- 755 Goovaerts, P. (1999). Geostatistics in soil science: state-of-the-art and perspectives. *Geoderma*, 89(1):1–
756 45.
- 757 Graham, A., Atkinson, P. M., and Danson, F. (2004). Spatial analysis for epidemiology. *Acta tropica*,
758 91(3):219–225.
- 759 Groemping, U. (2006). Relative importance for linear regression in R: The package relaimpo. *Journal of*
760 *Statistical Software*, 17(1):1–27.
- 761 Grossman, J. N., Grosz, A. E., Schweitzer, P. N., and Schruben, P. G. (2004). *The National Geochemical*
762 *Survey-database and documentation*. Open-File Report 2004-1001. USGS Eastern Mineral and
763 Environmental Resources Science Center.
- 764 Hartkamp, A. D., De Beurs, K., Stein, A., and White, J. W. (1999). Interpolation techniques for climate
765 variables.
- 766 Hengl, T. (2009). *A practical guide to geostatistical mapping*. Lulu, Amsterdam, the Netherlands.
- 767 Hengl, T., AghaKouchak, A., and Perčec Tadić, M. (2010). Methods and data sources for spatial prediction
768 of rainfall. In *Rainfall: State of the science*, pages 189–214. Wiley Online Library.
- 769 Hengl, T., Heuvelink, G. B., Kempen, B., Leenaars, J. G., Walsh, M. G., Shepherd, K. D., Sila, A.,
770 MacMillan, R. A., Mendes de Jesus, J., Tamene, L., and Tondoh, J. E. (2015). Mapping Soil Properties
771 of Africa at 250 m Resolution: Random Forests Significantly Improve Current Predictions. *PLoS ONE*,
772 10(e0125814).
- 773 Hengl, T., Heuvelink, G. B., and Rossiter, D. G. (2007a). About regression-kriging: from equations to
774 case studies. *Computers & Geosciences*, 33(10):1301–1315.
- 775 Hengl, T., Toomanian, N., Reuter, H. I., and Malakouti, M. J. (2007b). Methods to interpolate soil
776 categorical variables from profile observations: lessons from Iran. *Geoderma*, 140(4):417–427.
- 777 Hijmans, R. J. and van Etten, J. (2017). *raster: Geographic data analysis and modeling*. R package
778 version 2.6-7.
- 779 Hsiao, C. K., Juang, K.-W., and Lee, D.-Y. (2000). Estimating the second-stage sample size and the most
780 probable number of hot spots from a first-stage sample of heavy-metal contaminated soil. *Geoderma*,
781 95(1-2):73–88.
- 782 Hudson, G. and Wackernagel, H. (1994). Mapping temperature using kriging with external drift: theory
783 and an example from scotland. *International Journal of Climatology*, 14(1):77–91.
- 784 Isaaks, E. H. and Srivastava, R. M. (1989). *Applied Geostatistics*. Oxford University Press, New York.

- 785 Karger, D. N., Conrad, O., Böhner, J., Kawohl, T., Kreft, H., Soria-Auza, R. W., Zimmermann, N. E.,
786 Linder, H. P., and Kessler, M. (2017). Climatologies at high resolution for the earth's land surface areas.
787 *Scientific Data*, 4.
- 788 Knotters, M. and Brus, D. (2013). Purposive versus random sampling for map validation: a case study on
789 ecotope maps of floodplains in the netherlands. *Ecohydrology*, 6(3):425–434.
- 790 Kutner, M. H., Nachtsheim, C. J., Neter, J., and Li, W., editors (2004). *Applied Linear Statistical Models*.
791 McGraw-Hill, 5th edition.
- 792 Lark, R., Cullis, B., and Welham, S. (2006). On spatial prediction of soil properties in the presence of a
793 spatial trend: the empirical best linear unbiased predictor (E-BLUP) with REML. *European Journal of*
794 *Soil Science*, 57(6):787–799.
- 795 Latinne, P., Debeir, O., and Decaestecker, C. (2001). Limiting the number of trees in random forests.
796 *Multiple Classifier Systems*, pages 178–187.
- 797 Li, J. and Heap, A. D. (2011). A review of comparative studies of spatial interpolation methods in
798 environmental sciences: Performance and impact factors. *Ecological Informatics*, 6(3):228–241.
- 799 Lin, H. W., Tegmark, M., and Rolnick, D. (2017). Why does deep and cheap learning work so well?
800 *Journal of Statistical Physics*, 168(6):1223–1247.
- 801 Lopes, M. E. (2015). *Measuring the Algorithmic Convergence of Random Forests via Bootstrap Extrapolation*.
802 Department of Statistics, University of California, Davis CA.
- 803 Matheron, G. (1969). *Le krigeage universel*, volume 1. Cahiers du Centre de Morphologie Mathématique,
804 École des Mines de Paris, Fontainebleau.
- 805 McBratney, A., Santos, M. M., and Minasny, B. (2003). On digital soil mapping. *Geoderma*, 117(1):3–52.
- 806 Meerschman, E., Cockx, L., and Van Meirvenne, M. (2011). A geostatistical two-phase sampling strategy
807 to map soil heavy metal concentrations in a former war zone. *European Journal of Soil Science*,
808 62(3):408–416.
- 809 Meinshausen, N. (2006). Quantile regression forests. *Journal of Machine Learning Research*, 7:983–999.
- 810 Mentch, L. and Hooker, G. (2016). Quantifying uncertainty in random forests via confidence intervals
811 and hypothesis tests. *Journal of Machine Learning Research*, 17(1):841–881.
- 812 Meyer, H., Reudenbach, C., Hengl, T., Katurji, M., and Nauss, T. (2018). Improving performance of
813 spatio-temporal machine learning models using forward feature selection and target-oriented validation.
814 *Environmental Modelling & Software*, 101:1 – 9.
- 815 Miller, H. J. (2004). Tobler's first law and spatial analysis. *Annals of the Association of American*
816 *Geographers*, 94(2):284–289.
- 817 Minasny, B. and McBratney, A. B. (2007). Spatial prediction of soil properties using eblup with the
818 matérn covariance function. *Geoderma*, 140(4):324–336.
- 819 Moore, D. A. and Carpenter, T. E. (1999). Spatial analytical methods and geographic information systems:
820 use in health research and epidemiology. *Epidemiologic Reviews*, 21(2):143–161.
- 821 Nussbaum, M., Spiess, K., Baltensweiler, A., Grob, U., Keller, A., Greiner, L., Schaepman, M. E., and
822 Papritz, A. (2017a). Evaluation of digital soil mapping approaches with large sets of environmental
823 covariates. *SOIL Discussions*, 2017:1–32.
- 824 Nussbaum, M., Spiess, K., Baltensweiler, A., Grob, U., Keller, A., Greiner, L., Schaepman, M. E., and

- 825 Papritz, A. (2017b). Evaluation of digital soil mapping approaches with large sets of environmental
826 covariates. *SOIL Discuss*, pages 1–32.
- 827 Oliver, M. and Webster, R. (2014). A tutorial guide to geostatistics: Computing and modelling variograms
828 and kriging. *Catena*, 113:56–69.
- 829 Oliver, M. A. and Webster, R. (1990). Kriging: a method of interpolation for geographical information
830 systems. *International Journal of Geographical Information System*, 4(3):313–332.
- 831 Olson, R. S., La Cava, W., Mustahsan, Z., Varik, A., and Moore, J. H. (2017). Data-driven Advice for
832 Applying Machine Learning to Bioinformatics Problems. *ArXiv e-prints*.
- 833 Pebesma, E. J. (2004). Multivariable geostatistics in S: the gstat package. *Computers & Geosciences*,
834 30(7):683–691.
- 835 Pekel, J.-F., Cottam, A., Gorelick, N., and Belward, A. S. (2016). High-resolution mapping of global
836 surface water and its long-term changes. *Nature*, 504:418–422.
- 837 Prasad, A. M., Iverson, L. R., and Liaw, A. (2006). Newer classification and regression tree techniques:
838 bagging and random forests for ecological prediction. *Ecosystems*, 9(2):181–199.
- 839 Probst, P. and Boulesteix, A.-L. (2017). To tune or not to tune the number of trees in random forest?
840 *ArXiv e-prints*.
- 841 Ramcharan, A., Hengl, T., Nauman, T., Brungard, C., Waltman, S., Wills, S., and Thompson, J. (2018).
842 Soil property and class maps of the conterminous us at 100 meter spatial resolution based on a
843 compilation of national soil point observations and machine learning. *Soil Science Society of America
844 Journal*, 82:186–201.
- 845 Skøien, J. O., Merz, R., and Blöschl, G. (2005). Top-kriging? geostatistics on stream networks. *Hydrology
846 and Earth System Sciences Discussions*, 2(6):2253–2286.
- 847 Solow, A. R. (1986). Mapping by simple indicator kriging. *Mathematical Geology*, 18(3):335–352.
- 848 Strobl, C., Boulesteix, A.-L., Zeileis, A., and Hothorn, T. (2007). Bias in random forest variable
849 importance measures: Illustrations, sources and a solution. *BMC Bioinformatics*, 8(1):25.
- 850 van Etten, J. (2017). R package gdistance: Distances and routes on geographical grids. *Journal of
851 Statistical Software*, 76(13):1–21.
- 852 Vaysse, K. and Lagacherie, P. (2015). Evaluating digital soil mapping approaches for mapping Glob-
853 alSoilMap soil properties from legacy data in Languedoc-Roussillon (France). *Geoderma Regional*,
854 4:20–30.
- 855 Wager, S., Hastie, T., and Efron, B. (2014). Confidence intervals for random forests: the jackknife and the
856 infinitesimal jackknife. *Journal of Machine Learning Research*, 15(1):1625–1651.
- 857 Webster, R. and Oliver, M. A. (2001). *Geostatistics for Environmental Scientists*. Statistics in Practice.
858 Wiley, Chichester.
- 859 Wright, M. N. and Ziegler, A. (2017). ranger: A Fast Implementation of Random Forests for High
860 Dimensional Data in C++ and R. *Journal of Statistical Software*, 77(1):1–17.
- 861 Zhu, X., Vondrick, C., Ramanan, D., and Fowlkes, C. C. (2012). Do We Need More Training Data or
862 Better Models for Object Detection? In *BMVC*, volume 3, page 5.